

A Stochastic Proximal Polyak Step Size

Anonymous authors
Paper under double-blind review

Abstract

Recently, the stochastic Polyak step size (SPS) has emerged as a competitive adaptive step size scheme for stochastic gradient descent. Here we develop **ProxSPS**, a *proximal* variant of SPS that can handle regularization terms. Developing a proximal variant of SPS is particularly important, since SPS requires a lower bound of the objective function to work well. When the objective function is the sum of a loss and a regularizer, available estimates of a lower bound of the sum can be loose. In contrast, **ProxSPS** only requires a lower bound for the loss which is often readily available. As a consequence, we show that **ProxSPS** is easier to tune and more stable in the presence of regularization. Furthermore for image classification tasks, **ProxSPS** performs as well as **AdamW** with little to no tuning, and results in a network with smaller weight parameters. We also provide an extensive convergence analysis for **ProxSPS** that includes the non-smooth, smooth, weakly convex and strongly convex setting.

1 Introduction

Consider problems of the form

$$\min_{x \in \mathbb{R}^n} f(x), \quad f(x) := \mathbb{E}_P[f(x; S)] = \int_{\mathcal{S}} f(x; s) dP(s), \quad (1)$$

where \mathcal{S} is a sample space (or sample set). Formally, we can see S as a random variable mapping to \mathcal{S} and $P(s)$ as the associated probability measure. Let us assume that for each $s \in \mathcal{S}$, the function $f(\cdot; s) : \mathbb{R}^n \rightarrow \mathbb{R}$ is locally Lipschitz and hence possesses the Clarke subdifferential $\partial f(\cdot; s)$ (Clarke, 1983). Problems of form (1) arise in machine learning tasks where \mathcal{S} is the space of available data points (Bottou et al., 2018). An efficient method for such problems is stochastic (sub)gradient descent (Robbins & Monro, 1951; Bottou, 2010; Davis & Drusvyatskiy, 2019), given by

$$x^{k+1} = x^k - \alpha_k g_k, \quad g_k \in \partial f(x^k; S_k), \quad \text{where } S_k \sim P. \quad (\text{SGD})$$

Moreover, we will also consider the composite problem

$$\min_{x \in \mathbb{R}^n} \psi(x), \quad \psi(x) := f(x) + \varphi(x), \quad (2)$$

where $\varphi : \mathbb{R}^n \rightarrow \mathbb{R} \cup \{\infty\}$ is a proper, closed, and convex regularization function. In practical situations, the expectation in the objective function f is typically approximated by a sample average over $N \in \mathbb{N}$ data points. We formalize this special case with

$$\mathcal{S} = \{s_1, \dots, s_N\}, \quad P(s_i) = \frac{1}{N}, \quad f_i := f(\cdot; s_i) \quad i = 1, \dots, N. \quad (\text{ER})$$

In this case, problem (1) becomes the empirical risk minimization problem

$$\min_{x \in \mathbb{R}^n} \frac{1}{N} \sum_{i=1}^N f_i(x).$$

1.1 Background and Contributions

Polyak step size. For minimizing a convex, possibly non-differentiable function f , Polyak (1987, Chapter 5.3) proposed

$$x^{k+1} = x^k - \alpha_k g_k, \quad \alpha_k = \frac{f(x^k) - \min f}{\|g_k\|^2}, \quad g_k \in \partial f(x^k) \setminus \{0\}.$$

This particular choice of α_k , requiring the knowledge of $\min f$, has been subsequently called the *Polyak step size* for the subgradient method. Recently, Berrada et al. (2019); Loizou et al. (2021); Orvieto et al. (2022) adapted the Polyak step size to the stochastic setting: consider the (ER) case and assume that each f_i is differentiable and that a lower bound $C(s_i) \leq \inf_x f_i(x)$ is known for all $i \in [N]$. The method proposed by (Loizou et al., 2021) is

$$x^{k+1} = x^k - \min \left\{ \gamma_b, \frac{f_{i_k}(x^k) - C(s_{i_k})}{c \|\nabla f_{i_k}(x^k)\|^2} \right\} \nabla f_{i_k}(x^k), \quad (\text{SPS}_{\max})$$

with hyper-parameters $c, \gamma_b > 0$ and where in each iteration i_k is drawn from $\{1, \dots, N\}$ uniformly at random. It is important to note that the initial work (Loizou et al., 2021) used $C(s_i) = \inf f_i$; later, Orvieto et al. (2022) established theory for (SPS_{max}) for the more general case of $C(s_i) \leq \inf_x f_i(x)$ and allowing for mini-batching. Other works analyzed the Polyak step size in the convex, smooth setting (Hazan & Kakade, 2019) and in the convex, smooth and stochastic setting (Prazeres & Oberman, 2021). Further, the stochastic Polyak step size is closely related to stochastic model-based proximal point (Asi & Duchi, 2019) as well as stochastic bundle methods (Parens et al., 2022).

Contribution. We propose a proximal version of the stochastic Polyak step size, called ProxSPS, which explicitly handles regularization functions. Our proposal is based crucially on the fact that the stochastic Polyak step size can be motivated with stochastic proximal point for a truncated linear model of the objective function (we explain this in detail in Section 3.1). Our method has closed-form updates for squared ℓ_2 -regularization. We provide theoretical guarantees for ProxSPS for any closed, proper, and convex regularization function (including indicator functions for constraints). Our main results, Theorem 7 and Theorem 8, also give new insights for SPS_{max}, in particular showing exact convergence for convex and non-convex settings.

Lower bounds and regularization. Methods such as SPS_{max} need to estimate a lower bound $C(s)$ for each loss function $f(\cdot; s)$. Though $\inf_x f(x; s)$ can be precomputed in some restricted settings, in practice the lower bound $C(s) = 0$ is used for non-negative loss functions.¹ The tightness of the choice $C(s)$ is further reflected in the constant $\sigma^2 := \min f - \mathbb{E}_P[C(S)]$, which affects the convergence guarantees of SPS_{max} (Orvieto et al., 2022).

Contribution. For regularized problems (2) and if φ is differentiable, the current proposal of SPS_{max} would add φ to every loss function $f(\cdot; s)$. In this case, for non-negative regularization terms, such as the squared ℓ_2 -norm, the lower bound $C(s) = 0$ is always loose. Indeed, if $\varphi \geq 0$, then $\inf_{x \in \mathbb{R}^n} (f(x; s) + \varphi(x)) \geq \inf_{x \in \mathbb{R}^n} f(x; s)$ and this inequality is strict in most practical scenarios. For our proposed method ProxSPS, we now need only estimate a lower bound for the loss $f(x; s)$ and not for the composite function $f(x; s) + \varphi(x)$. Further, ProxSPS decouples the adaptive step size for the gradient of the loss from the regularization (we explain this in detail in Section 4.1 and Fig. 1).

Proximal and adaptive methods. The question on how to handle regularization terms has also been posed for other families of adaptive methods. For Adam (Kingma & Ba, 2015) with ℓ_2 -regularization it has been observed that it generalizes worse and is harder to tune than AdamW (Loshchilov & Hutter, 2019) which uses weight decay. Further, AdamW can be seen as an approximation to a proximal version of Adam (Zhuang et al., 2022).² On the other hand, Loizou et al. (2021) showed that – without regularization – default hyperparameter settings for SPS_{max} give very encouraging results on matrix factorization and image classification tasks. This is promising since it suggests that SPS_{max} is an *adaptive* method, and can work well across varied tasks without the need for extensive hyperparameter tuning.

¹See for instance <https://github.com/IssamLaradji/spa>.

²For SGD treating ℓ_2 -regularization as a part of the loss can be seen to be equivalent to its proximal version (cf. Appendix C).

Contribution. We show that by handling ℓ_2 -regularization using a proximal step, our resulting ProxSPS is less sensitive to hyperparameter choice as compared to SPS_{max}. This becomes apparent in matrix factorization problems, where ProxSPS converges for a much wider range of regularization parameters and learning rates, while SPS_{max} is more sensitive to these settings. We also show similar results for image classification over the CIFAR10 dataset when using a ResNet56 and ResNet110 model, where we also compare our method to AdamW.

The remainder of our paper is organized as follows: we will first recall how the stochastic Polyak step size, in the case of $\varphi = 0$, can be derived using the model-based approach of (Asi & Duchi, 2019; Davis & Drusvyatskiy, 2019) and how this is connected to SPS_{max}. We then derive ProxSPS based on the connection to model-based methods, and present our theoretical results, based on the proof techniques in (Davis & Drusvyatskiy, 2019).

2 Preliminaries

2.1 Notation

Throughout, we will write \mathbb{E} instead of \mathbb{E}_P . For any random variable $X(s)$, we denote $\mathbb{E}[X(S)] := \int_S X(s)dP(s)$. We denote $(\cdot)_+ := \max\{\cdot, 0\}$. We write $\tilde{\mathcal{O}}$ when we drop logarithmic terms in the \mathcal{O} -notation, e.g. $\tilde{\mathcal{O}}(\frac{1}{K}) = \mathcal{O}(\frac{\ln(1+K)}{K})$.

2.2 General assumptions

Throughout the article, we assume the following:

Assumption 1. *It is possible to generate infinitely many i.i.d. realizations S_1, S_2, \dots from \mathcal{S} .*

Assumption 2. *For every $s \in \mathcal{S}$, $\inf_x f(x; s)$ is finite and there exists $C(s)$ satisfying $C(s) \leq \inf_x f(x; s)$.*

In many machine learning applications, non-negative loss functions are used and thus we can satisfy the second assumption choosing $C(s) = 0$ for all $s \in \mathcal{S}$.

2.3 Convex analysis

Let $h : \mathbb{R}^n \rightarrow \mathbb{R}$ be convex and $\alpha > 0$. The proximal operator is given by

$$\text{prox}_{\alpha h}(x) := \arg \min_y h(y) + \frac{1}{2\alpha} \|y - x\|^2.$$

Further, the Moreau envelope is defined by $\text{env}_h^\alpha(x) := \min_y h(y) + \frac{1}{2\alpha} \|y - x\|^2$, and its derivative is $\nabla \text{env}_h^\alpha(x) = \frac{1}{\alpha}(x - \text{prox}_{\alpha h}(x))$ (Drusvyatskiy & Paquette, 2019, Lem. 2.1). Moreover, due to the optimality conditions of the proximal operator, if $h \in \mathcal{C}^1$ then

$$\hat{x} = \text{prox}_{\alpha h}(x) \implies \|\nabla h(\hat{x})\| = \alpha^{-1} \|x - \hat{x}\| = \|\nabla \text{env}_h^\alpha(x)\|. \quad (3)$$

Davis & Drusvyatskiy (2019) showed how to use the Moreau envelope as a measure of stationarity: if $\|\nabla \text{env}_h^\alpha(x)\|$ is small, then x is close to \hat{x} and \hat{x} is an almost stationary point of h . Formally, the gradient of the Moreau envelope can be related to the gradient mapping (cf. (Drusvyatskiy & Paquette, 2019, Thm. 4.5) and Lemma 11).

We say that a function $h : \mathbb{R}^n \rightarrow \mathbb{R}$ is L -smooth if its gradient is L -Lipschitz, that is

$$\|\nabla h(x) - \nabla h(y)\| \leq L \|x - y\|, \quad \forall x, y \in \mathbb{R}^n. \quad (4)$$

If h is L -smooth, then

$$h(y) \leq h(x) + \langle \nabla h(x), y - x \rangle + \frac{L}{2} \|y - x\|^2 \quad \text{for all } x, y \in \mathbb{R}^n.$$

A function $h : \mathbb{R}^n \rightarrow \mathbb{R}$ is ρ -weakly convex for $\rho \geq 0$ if $h + \frac{\rho}{2}\|\cdot\|^2$ is convex. Any L -smooth function is weakly convex with parameter less than or equal to L (Drusvyatskiy & Paquette, 2019, Lem. 4.2). The above results on the proximal operator and Moreau envelope can immediately be extended to h being ρ -weakly convex if $\alpha \in (0, \rho^{-1})$, since then $h + \frac{\rho}{2}\|\cdot\|^2$ is convex.

If we assume that each $f(\cdot; s)$ is ρ_s -weakly convex for $\rho_s \geq 0$, then applying (Bertsekas, 1973, Lem. 2.1) to the convex function $f(\cdot; s) + \frac{\rho_s}{2}\|\cdot\|^2$ yields that $f + \frac{\rho}{2}\|\cdot\|^2$ is convex and thus f is ρ -weakly convex for $\rho := \mathbb{E}[\rho_s]$. In particular, f is convex if each $f(\cdot; s)$ is assumed to be convex. For a weakly convex function h , we denote with ∂h the regular subdifferential (cf. (Davis & Drusvyatskiy, 2019, section 2.2) and (Rockafellar & Wets, 1998, Def. 8.3)).

3 The unregularized case

For this section, consider problems of form (1), i.e. no regularization term φ is added to the loss f .

3.1 A model-based view point

Many classical methods for solving (1) can be summarized by model-based stochastic proximal point: in each iteration, a model $f_x(\cdot; s)$ is constructed approximating $f(\cdot; s)$ locally around x . With $S_k \sim P$ being drawn at random, this yields the update

$$x^{k+1} = \arg \min_{y \in \mathbb{R}^n} f_x(y; S_k) + \frac{1}{2\alpha_k} \|y - x^k\|^2. \quad (5)$$

The theoretical foundation for this family of methods has been established by Asi & Duchi (2019) and Davis & Drusvyatskiy (2019). They give the following three models as examples:

- (i) *Linear*: $f_x(y; s) := f(x; s) + \langle g, y - x \rangle$ with $g \in \partial f(x; s)$.
- (ii) *Full*: $f_x(y; s) := f(y; s)$.
- (iii) *Truncated*: $f_x(y; s) := \max\{f(x; s) + \langle g, y - x \rangle, \inf_{z \in \mathbb{R}^n} f(z; s)\}$ where $g \in \partial f(x; s)$.

It is easy to see that update (5) for the *linear model* is equal to (SGD) while the *full model* results in the stochastic proximal point method. For the *truncated model*, (5) results in the update

$$x^{k+1} = x^k - \min \left\{ \alpha_k, \frac{f(x^k; S_k) - \inf_{z \in \mathbb{R}^n} f(z; S_k)}{\|g_k\|^2} \right\} g_k, \quad g_k \in \partial f(x^k; S_k). \quad (6)$$

More generally, one can replace the term $\inf_{x \in \mathbb{R}^n} f(x; S_k)$ with an arbitrary lower bound of $f(\cdot; S_k)$ (cf. Lemma 10). The model-based stochastic proximal point method for the truncated model is given in Algorithm 1. The connection between the truncated model and the method depicted in (6) is not a new insight and has been pointed out in several works (including (Asi & Duchi, 2019; Loizou et al., 2021) and (Berrada et al., 2019, Prop. 1)). For simplicity, we refer to Algorithm 1 as SPS throughout this article. However, it should be pointed out that this acronym (and variations of it) have been used for stochastic Polyak-type methods in slightly different ways (Loizou et al., 2021; Gower et al., 2021).

Algorithm 1 SPS

Require: $x^0 \in \mathbb{R}^n$, step sizes $\alpha_k > 0$.

for $k = 0, 1, 2, \dots, K - 1$ **do**

1. Sample S_k and set $C_k := C(S_k)$.
2. Choose $g_k \in \partial f(x^k; S_k)$. If $g_k = 0$, set $x^{k+1} = x^k$. Otherwise, set

$$x^{k+1} = x^k - \gamma_k g_k, \quad \gamma_k = \min \left\{ \alpha_k, \frac{f(x^k; S_k) - C_k}{\|g_k\|^2} \right\}. \quad (7)$$

return x^K

For instance consider again the SPS_{\max} method

$$x^{k+1} = x^k - \min \left\{ \gamma_b, \frac{f_{i_k}(x^k) - C(s_{i_k})}{c \|\nabla f_{i_k}(x^k)\|^2} \right\} \nabla f_{i_k}(x^k), \quad (\text{SPS}_{\max})$$

where $c, \gamma_b > 0$. Clearly, for $c = 1$ and $\alpha_k = \gamma_b$, update (7) is identical to SPS_{\max} . With this in mind, we can interpret the hyperparameter γ_b in SPS_{\max} simply as a step size for the model-based stochastic proximal point step. For the parameter c on the other hand, the model-based approach motivates the choice $c = 1$. In this article, we will focus on this natural choice $c = 1$ which also reduces the amount of hyperparameter tuning. However, we should point out that, in the strongly convex case, $c = 1/2$ gives the best rate of convergence in (Loizou et al., 2021).

4 The regularized case

Now we consider regularized problems of the form (2), i.e.

$$\min_{x \in \mathbb{R}^n} \psi(x), \quad \psi(x) = f(x) + \varphi(x),$$

where $\varphi : \mathbb{R}^n \rightarrow \mathbb{R} \cup \{\infty\}$ is a proper, closed, λ -strongly convex function for $\lambda \geq 0$ (we allow $\lambda = 0$). For $s \in \mathcal{S}$, denote by $\psi_x(\cdot; s)$ a stochastic model of the objective ψ at x . We aim to analyze algorithms with the update

$$x^{k+1} = \arg \min_{x \in \mathbb{R}^n} \psi_{x^k}(x; S_k) + \frac{1}{2\alpha_k} \|x - x^k\|^2, \quad (8)$$

where $S_k \sim P$ and $\alpha_k > 0$. Naively, if we know a lower bound $\tilde{C}(s)$ of $f(\cdot; s) + \varphi(\cdot)$, the truncated model could be constructed for the function $f(x; s) + \varphi(x)$, resulting in

$$\psi_x(y; s) = \max\{f(x; s) + \varphi(x) + \langle g + u, y - x \rangle, \tilde{C}(s)\}, \quad g \in \partial f(x; s), \quad u \in \partial \varphi(x). \quad (9)$$

In fact, Asi & Duchi (2019) and Loizou et al. (2021) work in the setting of unregularized problems and hence their approaches would handle regularization in this way. What we propose instead, is to only truncate a linearization of the loss $f(x; s)$, yielding the model

$$\psi_x(y; s) = f_x(y; s) + \varphi(y), \quad f_x(y; s) = \max\{f(x; s) + \langle g, y - x \rangle, C(s)\}, \quad g \in \partial f(x; s). \quad (10)$$

Solving (8) with the model in (10) results in

$$x^{k+1} = \arg \min_{y \in \mathbb{R}^n} \max\{f(x^k; S_k) + \langle g_k, y - x^k \rangle, C(S_k)\} + \varphi(y) + \frac{1}{2\alpha_k} \|y - x^k\|^2. \quad (11)$$

The resulting model-based stochastic proximal point method is given in Algorithm 2³. Lemma 12 shows that, if prox_φ is known, update (11) can be computed by minimizing a strongly convex function over a compact one-dimensional interval. The relation to the proximal operator of φ motivates the name ProxSPS. Further, the ProxSPS update (11) has a closed form solution when φ is the squared ℓ_2 -norm, as we detail in the next section.

Algorithm 2 ProxSPS

Require: $x^0 \in \mathbb{R}^n$, step sizes $\alpha_k > 0$.

for $k = 0, 1, 2, \dots, K - 1$ **do**

1. Sample S_k and set $C_k := C(S_k)$.
2. Choose $g_k \in \partial f(x^k; S_k)$.
- Update x^{k+1} according to (11).

return x^K

³For $\varphi = 0$, Algorithm 2 is identical to Algorithm 1.

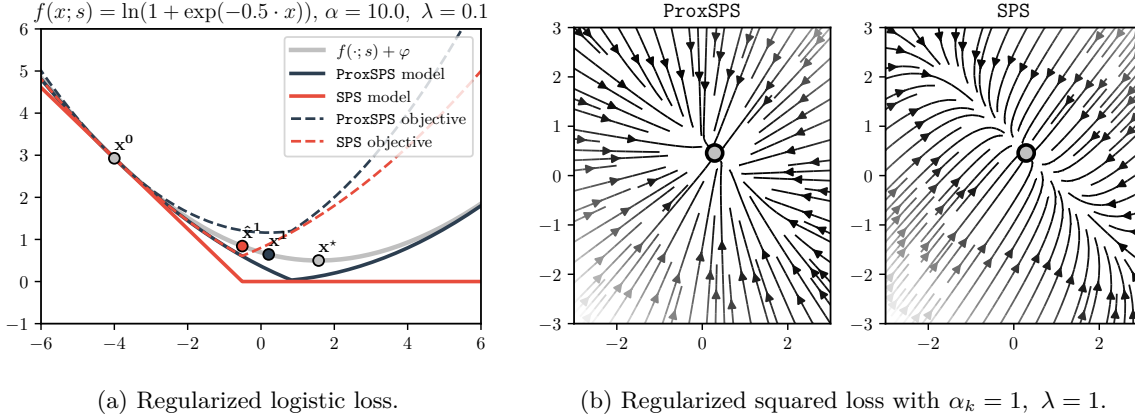


Figure 1: a) SPS refers to model (9) whereas ProxSPS refers to (10). We plot the corresponding model $\psi_{x^0}(y; s)$ and the objective function of (8). x^1 (resp. \hat{x}^1) denotes the new iterate for ProxSPS (resp. SPS), x^* is the minimizer of $f(\cdot; s) + \varphi$. b) Streamlines of the vector field $V(x^k) := x^{k+1} - x^k$, for $f(x) = \|Ax - b\|^2$ and for the deterministic update, i.e. $f(x; s) = f(x)$. ProxSPS refers to update (14) and SPS refers to (13). The circle marks the minimizer of $f(x) + \frac{\lambda}{2}\|x\|^2$.

4.1 The special case of ℓ_2 -regularization

When $\varphi(x) = \frac{\lambda}{2}\|x\|^2$ for some $\lambda > 0$, ProxSPS (11) has a closed form solution as we show next in Lemma 1. For this lemma, recall that the proximal operator of $\varphi(x) = \frac{\lambda}{2}\|x\|^2$ is given by $\text{prox}_{\alpha\varphi}(x) = \frac{1}{1+\alpha\lambda}x$ for all $\alpha > 0$, $x \in \mathbb{R}^n$.

Lemma 1. Let $\varphi(x) = \frac{\lambda}{2}\|x\|^2$ and let $g \in \partial f(x; s)$ and $C(s) \leq \inf_{z \in \mathbb{R}^n} f(z; s)$ hold for all $s \in \mathcal{S}$. For $\psi_x(y; s) = f_x(y; s) + \varphi(y)$ with $f_x(y; s) = \max\{f(x; s) + \langle g, y - x \rangle, C(s)\}$ consider the update

$$x^{k+1} = \arg \min_{x \in \mathbb{R}^n} \psi_{x^k}(x; S_k) + \frac{1}{2\alpha_k} \|x - x^k\|^2.$$

Denote $C_k := C(S_k)$ and let $g_k \in \partial f(x^k; S_k)$. Define

$$\tau_k^+ := \begin{cases} 0 & \text{if } g_k = 0, \\ \min \left\{ \alpha_k, \left(\frac{(1+\alpha_k\lambda)(f(x^k; S_k) - C_k) - \alpha_k\lambda \langle g_k, x^k \rangle}{\|g_k\|^2} \right)_+ \right\} & \text{else.} \end{cases}$$

Update (11) is given by

$$x^{k+1} = \frac{1}{1 + \alpha_k \lambda} \left(x^k - \tau_k^+ g_k \right) = \text{prox}_{\alpha_k \varphi}(x^k - \tau_k^+ g_k). \quad (12)$$

See Lemma 9 in the appendix for an extended version of the above lemma and its proof. The update (12) can be naturally decomposed into two steps, one stochastic gradient step with an adaptive stepsize, that is $\bar{x}^{k+1} = x^k - \tau_k^+ g_k$ followed by a proximal step $x^{k+1} = \text{prox}_{\alpha_k \varphi}(\bar{x}^{k+1})$. This decoupling into two steps, makes it easier to interpret the effect of each step, with τ_k^+ adjusting for the scale/curvature and the following proximal step shrinking the resulting parameters. There is no clear separation of tasks if we apply the SPS method to the regularized problem, as we see next.

Algorithm 3 ProxSPS for $\varphi = \frac{\lambda}{2} \|\cdot\|^2$

Require: $x^0 \in \mathbb{R}^n$, step sizes $\alpha_k > 0$.

for $k = 0, 1, 2, \dots, K - 1$ **do**

 1. Sample S_k and set $C_k := C(S_k)$.

 2. Choose $g_k \in \partial f(x^k; S_k)$. If $g_k = 0$, set $x^{k+1} = \frac{1}{1+\alpha_k\lambda}x^k$. Otherwise, set

$$x^{k+1} = \frac{1}{1+\alpha_k\lambda} \left[x^k - \min \left\{ \alpha_k, \left(\frac{(1+\alpha_k\lambda)(f(x^k; S_k) - C_k) - \alpha_k\lambda \langle g_k, x^k \rangle}{\|g_k\|^2} \right)_+ \right\} g_k \right].$$

return x^K

4.2 Comparing the model of SPS and ProxSPS

For simplicity, assume again the discrete sample space setting (ER) with differentiable loss functions f_i and let $\varphi = \frac{\lambda}{2} \|\cdot\|^2$. Clearly, the composite problem (2) can be transformed to an instance of (1) by setting $\ell_i(x) := f_i(x) + \frac{\lambda}{2} \|x\|^2$ and solving $\min_x \ell(x)$ with $\ell(x) := \frac{1}{N} \sum_{i=1}^N \ell_i(x)$. Assume that a lower bound $\underline{\ell}_i \leq \inf_x \ell_i(x)$ is known. In this case (9) becomes

$$\psi_x(y; s_i) = \max \left\{ f_i(x) + \frac{\lambda}{2} \|x\|^2 + \langle \nabla f_i(x) + \lambda x, y - x \rangle, \underline{\ell}_i \right\}.$$

Due to Lemma 10, if $\nabla f_{i_k}(x^k) + \lambda x^k \neq 0$, the update (8) is given by

$$x^{k+1} = x^k - \min \left\{ \alpha_k, \frac{f_{i_k}(x^k) + \frac{\lambda}{2} \|x^k\|^2 - \underline{\ell}_{i_k}}{\|\nabla f_{i_k}(x^k) + \lambda x^k\|^2} \right\} (\nabla f_{i_k}(x^k) + \lambda x^k). \quad (13)$$

We refer to this method, which is using model (9), as SPS. On the other hand, using model (10) and if $\nabla f_{i_k}(x^k) \neq 0$, the update of ProxSPS (12) is

$$x^{k+1} = \frac{1}{1+\alpha_k\lambda} \left[x^k - \min \left\{ \alpha_k, \left(\frac{(1+\alpha_k\lambda)(f_{i_k}(x^k) - C(s_{i_k})) - \alpha_k\lambda \langle \nabla f_{i_k}(x^k), x^k \rangle}{\|\nabla f_{i_k}(x^k)\|^2} \right)_+ \right\} \nabla f_{i_k}(x^k) \right]. \quad (14)$$

In Fig. 1a, we illustrate the two models (9) (denoted by SPS) and (10) (denoted by ProxSPS) for the logistic loss with squared ℓ_2 -regularization. We can see that the ProxSPS model is a much better approximation of the (stochastic) objective function as it still captures the quadratic behaviour of φ . Furthermore, as noted in the previous section, ProxSPS decouples the step size of the gradient and of the shrinkage, and hence the update direction depends on α_k . In contrast, the update direction of SPS does not depend on α_k , and the regularization effect is intertwined with the adaptive step size. Another way to see that the model (10) on which ProxSPS is based on is a more accurate model as compared to the SPS model (9), is that the resulting vector field of ProxSPS takes a more direct route to the minimum, as illustrated in Fig. 1b.

Update (14) needs to compute the term $\langle \nabla f_{i_k}(x^k), x^k \rangle$ while (13) needs to evaluate $\|x^k\|^2$. Other than that, the computational costs are roughly identical. For (14), a lower bound $\underline{\ell}_i$ is required. For non-negative loss functions, in practice both $\underline{\ell}_i$ and $C(s_i)$ are often set to zero, in which case (10) will be a more accurate model as compared to (9). ⁴

4.3 Convergence analysis

For the convergence analysis of Algorithm 2, we can work with the following assumption on φ .

Assumption 3. $\varphi : \mathbb{R}^n \rightarrow \mathbb{R} \cup \{\infty\}$ is a proper, closed, λ -strongly convex function with $\lambda \geq 0$.

⁴For single element sampling, $\inf \underline{\ell}_i$ can sometimes be precomputed (e.g. regularized logistic regression, see (Loizou et al., 2021, Appendix D)). But even in this restricted setting it is not clear how to estimate $\inf \underline{\ell}_i$ when using mini-batching.

Throughout this section we consider model (10), i.e. for $g \in \partial f(x; s)$, let

$$\psi_x(y; s) = f_x(y; s) + \varphi(y), \quad f_x(y; s) = \max\{f(x; s) + \langle g, y - x \rangle, C(s)\}.$$

Let us first state a lemma on important properties of the truncated model:

Lemma 2. *Consider $f_x(y; s) = \max\{f(x; s) + \langle g, y - x \rangle, C(s)\}$, where $g \in \partial f(x; s)$ is arbitrary and $C(s) \leq \inf_{z \in \mathbb{R}^n} f(z; s)$. Then, it holds:*

(i) *The mapping $y \mapsto f_x(y; s)$ is convex.*

(ii) *For all $x \in \mathbb{R}^n$, it holds $f_x(x; s) = f(x; s)$. If $f(\cdot; s)$ is ρ_s -weakly convex for all $s \in \mathcal{S}$, then*

$$f_x(y; s) \leq f(y; s) + \frac{\rho_s}{2} \|y - x\|^2 \quad \text{for all } x, y \in \mathbb{R}^n.$$

Proof. (i) The maximum over a constant and linear term is convex.

(ii) Recall that $C(s) \leq f(y; s)$ for all $y \in \mathbb{R}^n$. Therefore, $f_x(x; s) = \max\{C(s), f(x; s)\} = f(x; s)$. From weak convexity of $f(\cdot; s)$ it follows $f(x; s) + \langle g, y - x \rangle \leq f(y; s) + \frac{\rho_s}{2} \|y - x\|^2$ and therefore

$$f_x(y; s) \leq \max\{C(s), f(y; s) + \frac{\rho_s}{2} \|y - x\|^2\} = f(y; s) + \frac{\rho_s}{2} \|y - x\|^2 \quad \text{for all } y \in \mathbb{R}^n.$$

□

4.3.1 Globally bounded subgradients

In this section, we show that the results for stochastic model-based proximal point methods in Davis & Drusvyatskiy (2019) can be immediately applied to our specific model – even though this model has not been explicitly analyzed in their article. This, however, requires assuming that the subgradients are bounded.

Proposition 3. *Let Assumption 3 hold and assume that there is an open, convex set U containing $\text{dom } \varphi$. Let $f(\cdot; s)$ be ρ_s -weakly convex for all $s \in \mathcal{S}$ and let $\rho = \mathbb{E}[\rho_S]$. Assume that there exists $G_s \in \mathbb{R}_+$ for all $s \in \mathcal{S}$, such that $G := \sqrt{\mathbb{E}[G_s^2]} < \infty$ and*

$$\|g(x; s)\| \leq G_s \quad \forall g(x; s) \in \partial f(x; s), \quad \forall x \in U. \quad (15)$$

Then, $\psi_x(y; s)$ satisfies (Davis & Drusvyatskiy, 2019, Assum. B).

Proof. We verify properties (B1)–(B4) of (Davis & Drusvyatskiy, 2019, Assum. B), for $r = \varphi$ and $f_x(\cdot; \xi) = f_x(\cdot; s)$: (B1) is identical to Assumption 1. (B2) holds with $\tau = \rho$ due to our assumptions on φ , and Lemma 2, (ii) and the definition of f , i.e. $f(x) = \mathbb{E}[f(x; S)]$. Due to Lemma 2, (i) and convexity of φ , the mapping $f_x(\cdot; s) + \varphi(\cdot)$ is convex which shows (B3) for $\eta = 0$. Now, for arbitrary $g \in \partial f(x; s)$ and $x, y \in U$, we have

$$f_x(x; s) - f_x(y; s) \leq f(x; s) - f(x; s) - \langle g, y - x \rangle \leq \|g\| \|y - x\| \leq G_s \|y - x\|.$$

Hence, (B4) holds for $L = G$ and $L(\xi) = G_s$. □

Corollary 4 (Weakly convex case). *Let the assumptions of Proposition 3 hold with $\rho_s > 0$ for all $s \in \mathcal{S}$. Let $\rho = \mathbb{E}[\rho_S] < \infty$ and let $\Delta \geq \text{env}_\psi^{1/(2\rho)}(x^0) - \min \psi$. Let $\{x^k\}_{k=0, \dots, K}$ be generated by Algorithm 2 for constant step sizes $\alpha_k = \left(2\rho + \sqrt{\frac{4\rho G^2 K}{\Delta}}\right)^{-1}$. Then, it holds*

$$\mathbb{E}\|\nabla \text{env}_\psi^{1/(2\rho)}(x_\sim^K)\|^2 \leq \frac{8\rho\Delta}{K} + 16G\sqrt{\frac{\rho\Delta}{K}},$$

where x_\sim^K is uniformly drawn from $\{x^0, \dots, x^{K-1}\}$.

Proof. The claim follows from Proposition 3 and (Davis & Drusvyatskiy, 2019, Thm. 4.3), (4.16) setting $\eta = 0$, $\bar{\rho} = 2\rho$, $T = K - 1$ and $\beta_t = \alpha_k^{-1}$. □

Corollary 5 ((Strongly) convex case). *Let the assumptions of Proposition 3 hold with $\rho_s = 0$ for all $s \in \mathcal{S}$. Let $\lambda > 0$ and $x^* = \arg \min_x \psi(x)$. Let $\{x^k\}_{k=0,\dots,K}$ be generated by Algorithm 2 for step sizes $\alpha_k = \frac{2}{\lambda(k+1)}$. Then, it holds*

$$\mathbb{E} \left[\psi \left(\frac{2}{(K+1)(K+2)-2} \sum_{k=1}^K (k+1)x^k \right) - \psi(x^*) \right] \leq \frac{\lambda}{(K+1)^2} \|x^0 - x^*\|^2 + \frac{8G^2}{\lambda(K+1)}.$$

Proof. As $\rho_s = 0$ and hence $\rho = 0$, from the proof of Proposition 3 we have that (Davis & Drusvyatskiy, 2019, Assum. B) is satisfied with $\tau = 0$ (in the notation of (Davis & Drusvyatskiy, 2019)). Moreover, by Lemma 2, (i) and λ -strong convexity of φ , we have λ -strong convexity of $\psi_x(\cdot; s)$. The claim follows from Proposition 3 and (Davis & Drusvyatskiy, 2019, Thm. 4.5) setting $\mu = \lambda$, $T = K - 1$ and $\beta_t = \alpha_k^{-1}$. \square

4.3.2 Lipschitz smoothness

Assumption (15), i.e. having globally bounded subgradients, is strong: it implies Lipschitz continuity of f (cf. (Davis & Drusvyatskiy, 2019, Lem. 4.1)) and simple functions such as the squared loss do not satisfy this. Therefore, we provide additional guarantees for the smooth case, without the assumption of globally bounded gradients.

The following result, similar to (Davis & Drusvyatskiy, 2019, Lem. 4.2), is the basic inequality for the subsequent convergence analysis.

Lemma 6. *Let Assumption 3 hold. Let x^{k+1} be given by (11) and ψ_{x^k} be given in (10). For every $x \in \mathbb{R}^n$ it holds*

$$(1 + \alpha_k \lambda) \|x^{k+1} - x\|^2 \leq \|x^k - x\|^2 - \|x^{k+1} - x^k\|^2 + 2\alpha_k (\psi_{x^k}(x; S_k) - \psi_{x^k}(x^{k+1}; S_k)). \quad (16)$$

Moreover, it holds

$$\psi_{x^k}(x^{k+1}; S_k) \geq f(x^k; S_k) + \langle g_k, x^{k+1} - x^k \rangle + \varphi(x^{k+1}). \quad (17)$$

Proof. The objective of (11) is given by $\Psi_k(y) := \psi_{x^k}(y; S_k) + \frac{1}{2\alpha_k} \|y - x^k\|^2$. Using Lemma 2, (i) and λ -strong convexity of φ , $\Psi_k(y)$ is $(\lambda + \frac{1}{\alpha_k})$ -strongly convex. As x^{k+1} is the minimizer of $\Psi_k(y)$, for all $x \in \mathbb{R}^n$ we have

$$\begin{aligned} \Psi_k(x) \geq \Psi_k(x^{k+1}) + \frac{1 + \alpha_k \lambda}{2\alpha_k} \|x^{k+1} - x\|^2 &\iff \\ (1 + \alpha_k \lambda) \|x^{k+1} - x\|^2 &\leq \|x^k - x\|^2 - \|x^{k+1} - x^k\|^2 + 2\alpha_k (\psi_{x^k}(x; S_k) - \psi_{x^k}(x^{k+1}; S_k)). \end{aligned}$$

Moreover, by definition of $f_x(y; s)$ in (10) we have

$$\psi_{x^k}(x^{k+1}; S_k) = f_{x^k}(x^{k+1}; S_k) + \varphi(x^{k+1}) \geq f(x^k; S_k) + \langle g_k, x^{k+1} - x^k \rangle + \varphi(x^{k+1}).$$

\square

We will work in the setting of differentiable loss functions with bounded gradient noise.

Assumption 4. *The mapping $f(\cdot; s)$ is differentiable for all $s \in \mathcal{S}$ and there exists $\beta \geq 0$ such that*

$$\mathbb{E} \|\nabla f(x; S) - \nabla f(x)\|^2 \leq \beta \quad \text{for all } x \in \mathbb{R}^n. \quad (18)$$

The assumption of bounded gradient noise (18) (in the differentiable setting) is indeed a weaker assumption than (15) since $\mathbb{E}[\nabla f(x; S)] = \nabla f(x)$ and

$$\mathbb{E} \|\nabla f(x; S) - \nabla f(x)\|^2 \leq \beta \iff \mathbb{E} \|\nabla f(x; S)\|^2 \leq \|\nabla f(x)\|^2 + \beta.$$

Remark 1. *Assumption 4* (and the subsequent theorems) could be adapted to the case where $f(\cdot; s)$ is weakly convex but non-differentiable: for fixed $x \in \mathbb{R}^n$, due to (Bertsekas, 1973, Prop. 2.2) and (Davis & Drusvyatskiy, 2019, Lem. 2.1) it holds

$$\mathbb{E}[\partial f(x; S)] = \mathbb{E}\left[\partial\left(f(x; S) + \frac{\rho_S}{2}\|x\|^2\right) - \rho_S x\right] = \partial f(x) + \rho x - \mathbb{E}[\rho_S x] = \partial f(x),$$

where we used $\rho = \mathbb{E}[\rho_S]$. Hence, for $g_s \in \partial f(x; s)$ we have $\mathbb{E}[g_s] \in \partial f(x)$ and (18) is replaced by

$$\mathbb{E}\|g_s - \mathbb{E}[g_s]\|^2 \leq \beta \quad \text{for all } x \in \mathbb{R}^n.$$

However, as we will still require that f is Lipschitz-smooth, we present our results for the differentiable setting.

The proof of the subsequent theorems can be found in Appendix A.2 and Appendix A.3.

Theorem 7. Let *Assumption 3* and *Assumption 4* hold. Let $f(\cdot; s)$ be convex for all $s \in \mathcal{S}$ and let f be L -smooth (4). Let $x^* = \arg \min_{x \in \mathbb{R}^n} \psi(x)$ and let $\theta > 1$. Let $\{x^k\}_{k=0,\dots,K}$ be generated by *Algorithm 2* for step sizes $\alpha_k > 0$ such that

$$\alpha_k \leq \frac{1 - 1/\theta}{L}. \quad (19)$$

Then, it holds

$$(1 + \alpha_k \lambda) \mathbb{E}\|x^{k+1} - x^*\|^2 \leq \mathbb{E}\|x^k - x^*\|^2 + 2\alpha_k \mathbb{E}[\psi(x^*) - \psi(x^{k+1})] + \theta\beta\alpha_k^2. \quad (20)$$

Moreover, we have:

a) If $\lambda > 0$ and $\alpha_k = \frac{1}{\lambda(k+k_0)}$ with $k_0 \geq 1$ large enough such that (19) is fulfilled, then

$$\mathbb{E}\left[\psi\left(\frac{1}{K} \sum_{k=0}^{K-1} x^{k+1}\right) - \psi(x^*)\right] \leq \frac{\lambda k_0}{2K} \|x^0 - x^*\|^2 + \frac{\theta\beta(1 + \ln K)}{2\lambda K}. \quad (21)$$

b) If $\lambda = 0$ and $\alpha_k = \frac{\alpha}{\sqrt{k+1}}$ with $\alpha \leq \frac{1-1/\theta}{L}$, then

$$\mathbb{E}\left[\psi\left(\frac{1}{\sum_{k=0}^{K-1} \alpha_k} \sum_{k=0}^{K-1} \alpha_k x^{k+1}\right) - \psi(x^*)\right] \leq \frac{\|x^0 - x^*\|^2}{4\alpha(\sqrt{K+1} - 1)} + \frac{\theta\beta\alpha(1 + \ln K)}{4(\sqrt{K+1} - 1)}. \quad (22)$$

c) If f is μ -strongly convex with $\mu \geq 0$,⁵ and $\alpha_k = \alpha$ fulfilling (19), then

$$\mathbb{E}\|x^K - x^*\|^2 \leq (1 + \alpha(\mu + 2\lambda))^{-K} \|x^0 - x^*\|^2 + \frac{\theta\beta\alpha}{\mu + 2\lambda}. \quad (23)$$

Remark 2. If $\lambda > 0$, for the decaying step sizes in item a) we get a rate of $\tilde{\mathcal{O}}(\frac{1}{K})$ if $\lambda > 0$. In the strongly convex case in item c), for constant step sizes, we get a linear convergence upto a neighborhood of the solution. Note that the constant on the right-hand side of (23) can be forced to be small using a small α . Further, the rate (23) has a 2λ term, instead of λ . This slight improvement in the rate occurs because we do not linearize φ in the ProxSPS model.

Theorem 8. Let *Assumption 3* and *Assumption 4* hold. Let $f(\cdot; s)$ be ρ_s -weakly convex for all $s \in \mathcal{S}$ and let $\rho := \mathbb{E}[\rho_S] < \infty$. Let f be L -smooth⁶ and assume that $\inf \psi > -\infty$. Let $\{x^k\}_{k \geq 0}$ be generated by *Algorithm 2*. For $\theta > 1$, under the condition

$$\eta \in \begin{cases} (0, \frac{1}{\rho - \lambda}) & \text{if } \rho > \lambda \\ (0, \infty) & \text{else} \end{cases}, \quad \alpha_k \leq \frac{1 - \theta^{-1}}{L + \eta^{-1}}, \quad (24)$$

⁵Note that as $f(\cdot; s)$ is convex, so is f , and that we allow $\mu = 0$ here.

⁶As f is ρ -weakly convex, this implies $\rho \leq L$.

it holds

$$\sum_{k=0}^{K-1} \alpha_k \mathbb{E} \|\nabla \text{env}_\psi^\eta(x^k)\|^2 \leq \frac{2(\text{env}_\psi^\eta(x^0) - \inf \psi)}{1 - \eta(\rho - \lambda)} + \frac{\beta\theta}{\eta(1 - \eta(\rho - \lambda))} \sum_{k=0}^{K-1} \alpha_k^2. \quad (25)$$

Moreover, for the choice $\alpha_k = \frac{\alpha}{\sqrt{k+1}}$ and with $\alpha \leq \frac{1-\theta^{-1}}{L+\eta^{-1}}$, we have

$$\min_{k=0, \dots, K-1} \mathbb{E} \|\nabla \text{env}_\psi^\eta(x^k)\|^2 \leq \frac{\text{env}_\psi^\eta(x^0) - \inf \psi}{\alpha(1 - \eta(\rho - \lambda))(\sqrt{K+1} - 1)} + \frac{\beta\theta}{2\eta(1 - \eta(\rho - \lambda))(\sqrt{K+1} - 1)} \frac{\alpha(1 + \ln K)}{(\sqrt{K+1} - 1)}.$$

If instead we choose $\alpha_k = \frac{\alpha}{\sqrt{K}}$ and with $\alpha \leq \sqrt{K} \frac{1-\theta^{-1}}{L+\eta^{-1}}$, we have

$$\mathbb{E} \|\nabla \text{env}_\psi^\eta(x_\sim^K)\|^2 \leq \frac{2(\text{env}_\psi^\eta(x^0) - \inf \psi)}{\alpha(1 - \eta(\rho - \lambda))\sqrt{K}} + \frac{\beta\theta}{\eta(1 - \eta(\rho - \lambda))} \frac{\alpha}{\sqrt{K}},$$

where x_\sim^K is uniformly drawn from $\{x^0, \dots, x^{K-1}\}$.

4.3.3 Comparison to existing theory

Recalling that [Algorithm 1](#) is equivalent to SPS_{\max} with $c = 1$ and $\gamma_b = \alpha_k$, we can apply [Theorem 7](#) and [Theorem 8](#) for the unregularized case where $\varphi = 0$ and hence obtain new theory for (SPS_{\max}) . We start by summarizing the main theoretical results for SPS_{\max} given in ([Loizou et al., 2021](#); [Orvieto et al., 2022](#)): in the [\(ER\)](#) setting, recall the interpolation constant $\sigma^2 = \mathbb{E}[f(x^*; S) - C(S)] = \frac{1}{N} \sum_{i=1}^N f_i(x^*) - C(s_i)$. If f_i is L_i -smooth and convex, ([Orvieto et al., 2022](#), Thm. 3.1) proves convergence to a neighborhood of the solution, i.e. the iterates $\{x^k\}$ of SPS_{\max} satisfy

$$\mathbb{E}[f(\bar{x}^K) - f(x^*)] \leq \frac{\|x^0 - x^*\|^2}{\alpha K} + \frac{2\gamma_b\sigma^2}{\alpha}, \quad (26)$$

where $\bar{x}^K := \frac{1}{K} \sum_{k=0}^{K-1} x^k$, $\alpha := \min\{\frac{1}{2cL_{\max}}, \gamma_b\}$, and $L_{\max} := \max_{i \in [N]} L_i$.⁷ For the nonconvex case, if f_i is L_i -smooth and under suitable assumptions on the gradient noise, ([Loizou et al., 2021](#), Thm. 3.8) states that, for constants c_1 and c_2 , we have

$$\min_{k=1, \dots, K} \mathbb{E} \|\nabla f(x^k)\|^2 \leq \frac{1}{c_1 K} + c_2. \quad (27)$$

The main advantage of these results is that γ_b can be held constant; furthermore in the convex setting (26), the choice of γ_b requires no knowledge of the smoothness constants L_i . For both results however, we can not directly conclude that the right-hand side goes to zero as $K \rightarrow \infty$ as there is an additional constant. Choosing γ_b sufficiently small does not immediately solve this as c_1 , α and c_2 all go to zero as γ_b goes to zero.

Our results complement this by showing exact convergence for the (weakly) convex convex case, i.e. without constants on the right-hand side. This comes at the cost of an upper bound on the step sizes α_k which depends on the smoothness constant L . For exact convergence, it is important to use decreasing step sizes α_k : [Theorem 8](#) shows that the gradient of the Moreau envelope converges to zero at the rate $\mathcal{O}(1/\sqrt{K})$ for the choice of $\alpha_k = \frac{\alpha}{\sqrt{K}}$.⁸ Another minor difference to ([Loizou et al., 2021](#)) is that we do not need to assume Lipschitz-smoothness for all $f(\cdot; s)$ and work instead with the (more general) assumption of weak convexity. However, we still need to assume Lipschitz smoothness of f .

Another variant of SPS_{\max} , named DecSPS , has been proposed in ([Orvieto et al., 2022](#)): for unregularized problems (1) it is given by

$$x^{k+1} = x^k - \hat{\gamma}_k g_k, \quad \hat{\gamma}_k = \frac{1}{c_k} \min \left\{ \frac{f(x^k; S_k) - C_k}{\|g_k\|^2}, c_{k-1} \hat{\gamma}_{k-1} \right\} \quad (\text{DecSPS})$$

⁷The theorem also handles the mini-batch case but, for simplicity, we state the result for sampling a single i_k in each iteration.

⁸Notice that α_k then depends on the total number of iterations K and hence one would need to fix K before starting the method.

where $\{c_k\}_{k \geq 0}$ is an increasing sequence. In the (ER) setting, if all f_i are Lipschitz-smooth and strongly convex, DecSPS converges with a rate of $\mathcal{O}(\frac{1}{\sqrt{K}})$, without knowledge of the smoothness or convexity constants (cf. (Orvieto et al., 2022, Thm. 5.5)). However, under these assumptions, the objective f is strongly convex and the optimal rate is $\mathcal{O}(\frac{1}{K})$, which we achieve up to a logarithmic factor in Theorem 7, (21). Moreover, for DecSPS no guarantees are given for nonconvex problems.

For regularized problems, the constant in (26) is problematic if σ^2 (computed for the regularized loss) is moderately large. We refer to Appendix D.3 where we show that this can easily happen - our results however do not depend on the size of σ^2 .

5 Numerical experiments

Throughout we denote Algorithm 1 with SPS and Algorithm 3 with ProxSPS. For all experiments we use PyTorch (Paszke et al., 2019).

5.1 General parameter setting

For SPS and ProxSPS we always use $C(s) = 0$ for all $s \in \mathcal{S}$. For α_k , we use the following schedules:

- **constant**: set $\alpha_k = \alpha_0$ for all k and some $\alpha_0 > 0$.
- **sqrt**: set $\alpha_k = \frac{\alpha_0}{\sqrt{j}}$ for all iterations k during epoch j .

As we consider problems with ℓ_2 -regularization, for SPS we handle the regularization term by incorporating it into all individual loss functions, as depicted in (13). With $\varphi = \frac{\lambda}{2}\|\cdot\|^2$ for $\lambda \geq 0$, we denote by ζ_k the *adaptive step size* term of the following algorithms:

- for SPS we have $\zeta_k := \frac{f(x^k; S_k) + \frac{\lambda}{2}\|x^k\|^2}{\|g_k + \lambda x^k\|^2}$ (cf. (13) with $\ell_{i_k} = 0$),
- for ProxSPS we have $\zeta_k := \left(\frac{(1+\alpha_k\lambda)f(x^k; S_k) - \alpha_k\lambda\langle g_k, x^k \rangle}{\|g_k\|^2} \right)_+$ and thus $\tau_k^+ = \min\{\alpha_k, \zeta_k\}$ (cf. Lemma 1 with $C(S_k) = 0$).

5.2 Regularized matrix factorization

Problem description: For $A \in \mathbb{R}^{q \times p}$, consider the problem

$$\min_{W_1 \in \mathbb{R}^{r \times p}, W_2 \in \mathbb{R}^{q \times r}} \mathbb{E}_{y \sim N(0, I)} \|W_2 W_1 y - A y\|^2 = \min_{W_1 \in \mathbb{R}^{r \times p}, W_2 \in \mathbb{R}^{q \times r}} \|W_2 W_1 - A\|_F^2.$$

For the above problem, SPS_{\max} has shown superior performance than other methods in the numerical experiments of (Loizou et al., 2021). The problem can be turned into a (nonconvex) empirical risk minimization problem by drawing N samples $\{y^{(1)}, \dots, y^{(N)}\}$. Denote $b^{(i)} := A y^{(i)}$. Adding squared norm regularization with $\lambda \geq 0$ (cf. (Srebro et al., 2004)), we obtain the problem

$$\min_{W_1 \in \mathbb{R}^{r \times p}, W_2 \in \mathbb{R}^{q \times r}} \frac{1}{N} \sum_{i=1}^N \|W_2 W_1 y^{(i)} - b^{(i)}\|^2 + \frac{\lambda}{2} (\|W_1\|_F^2 + \|W_2\|_F^2). \quad (28)$$

This is a problem of form (2), setting $x = (W_1, W_2)$, using a finite sample space $\mathcal{S} = \{s_1, \dots, s_N\}$, $f(x; s_i) = \|W_2 W_1 y^{(i)} - A y^{(i)}\|^2$, and $\varphi = \frac{\lambda}{2}\|\cdot\|_F^2$. Clearly, zero is a lower bound of $f(\cdot; s_i)$ for all $i \in [N]$.

We investigate ProxSPS for problems of form (28) on synthetic data. For details on the experimental procedure, we refer to Appendix D.1.

Discussion: We discuss the results for the setting `matrix-fac1` in Table 1 in the appendix. We first fix $\lambda = 0.001$ and consider the three methods SPS, ProxSPS and SGD. Fig. 2 shows the objective function over 50 epochs, for both step size schedules `sqrt` and `constant`, and several initial values α_0 . For the `constant`

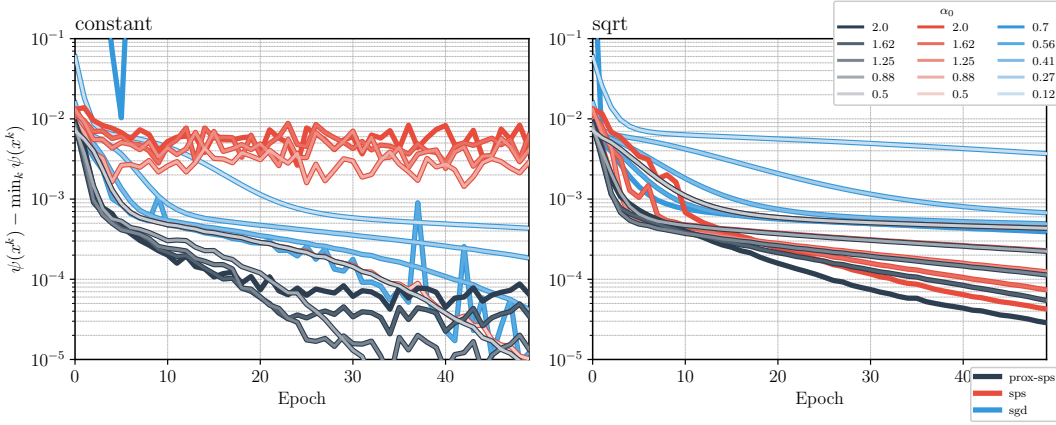


Figure 2: Objective function for the Matrix Factorization problem (28), with **constant** (left) and **sqrt** (right) step size schedule and several choices of initial values. Here $\min_k \psi(x^k)$ is the best objective function value found over all methods and all iterations.

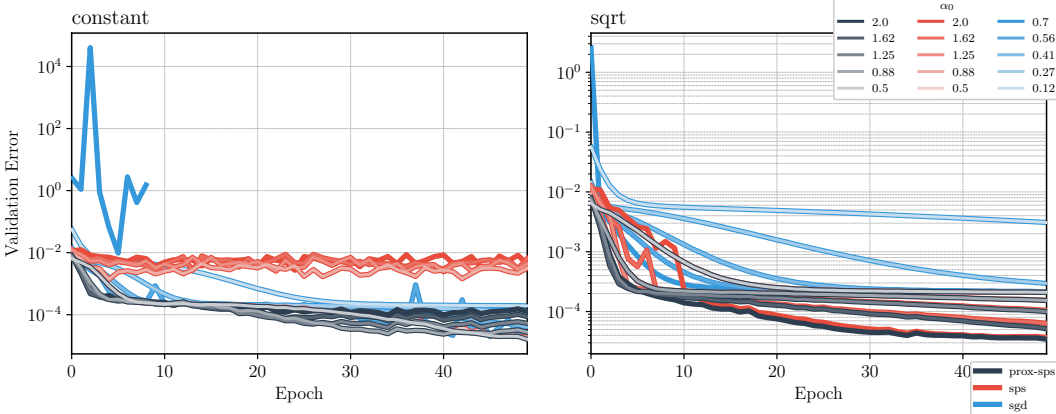


Figure 3: Validation error for the Matrix Factorization problem (28), with **constant** (left) and **sqrt** (right) step size schedule and several choices of initial values.

schedule, we observe that **ProxSPS** converges quickly for all initial values while **SPS** is unstable. Note that for **SGD** we need to pick much smaller values here in order to avoid divergence (**SGD** diverges for the largest value of α_0). Hence, **SPS** for large α_0 is unstable, while for small α_0 we can expect similar performance to **SGD** (as γ_k is capped by $\alpha_k = \alpha_0$). However, in the regime of small α_0 , convergence will be very slow. Hence, one of the main advantages of **SPS**, namely that its step size can be chosen constant and moderately large (compared to **SGD**), is not observed here. **ProxSPS** fixes this by admitting a large range of initial step sizes, which results in fast convergence, and therefore is more robust than **SGD** with respect to the tuning of α_0 .

For the **sqrt** schedule, we observe in Fig. 2 that **SPS** can be stabilized by reducing the values of α_k over the course of the iterations. However, for large α_0 we still see instability in the early iterations, whereas **ProxSPS** does not show this behaviour. We again observe that **ProxSPS** is less sensitive with respect to the choice of α_0 as compared to **SGD**. The empirical results also confirm our theoretical statement, showing exact convergence if α_k is decaying in the order of $1/\sqrt{k}$. From Fig. 3, we can make similar observations for the validation error, defined as $\frac{1}{N_{\text{val}}} \sum_{i=1}^{N_{\text{val}}} \|W_2 W_1 y^{(i)} - b_{\text{val}}^{(i)}\|^2$, where $b_{\text{val}}^{(i)}$ are the $N_{\text{val}} = N$ measurements from the validation set (cf. Appendix D.1 for details).

We now consider different values for λ and only consider the **sqrt** schedule, as we have seen that for constant step sizes, **SPS** would not work for large step sizes and be almost identical to **SGD** for small step sizes. Fig. 4

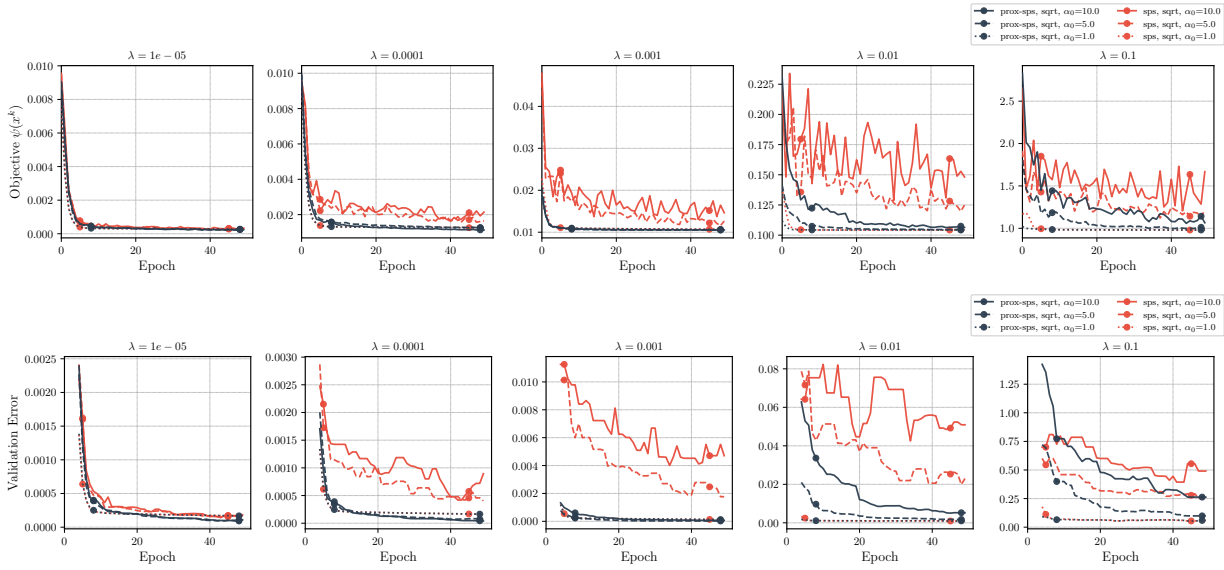


Figure 4: Objective function value and validation error over the course of optimization. For the validation error, we plot a rolling median over five epochs in order to avoid clutter.

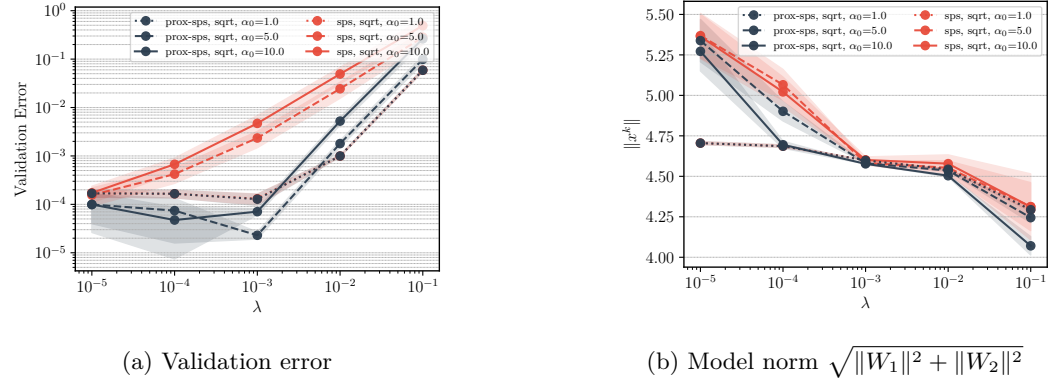


Figure 5: Validation error and model norm as a function of the regularization parameter λ . Shaded area is one standard deviation (computed over ten independent runs). For all values, we take the median over epochs [40, 50].

shows the objective function and validation error. Again, we can observe that SPS is unstable for large initial values α_0 for all $\lambda \geq 10^{-4}$. On the other hand, ProxSPS has a good performance for a wide range of $\alpha_0 \in [1, 10]$ if λ is not too large. Indeed, ProxSPS convergence only starts to deteriorate when both α_0 and λ are very large. For $\alpha_0 = 1$, the two methods give almost identical results. Finally, in Fig. 5a we plot the validation error as a function of λ (taking the median over the last ten epochs). The plot shows that the best validation error is obtained for $\lambda = 10^{-4}$ and for large α_0 . With SPS the validation error is higher, in particular for large α_0 and λ . Finally, we plot the actual step sizes for both methods in Fig. 6. We observe that the adaptive step size ζ_k (Definition at end of Section 5.1) is typically larger and has more variance for SPS than ProxSPS, in particular for large λ . This increased variance might explain why SPS is unstable when α_0 is large: the actual step size is the minimum between α_k and ζ_k and hence both terms being large could lead to instability. On the other hand, if $\alpha_0 = 1$, the plot confirms that SPS and ProxSPS are almost identical methods as $\zeta_k > \alpha_k$ for most iterations. We plot the results for the setting `matrix-fac2` of Table 1 in Appendix D.2.

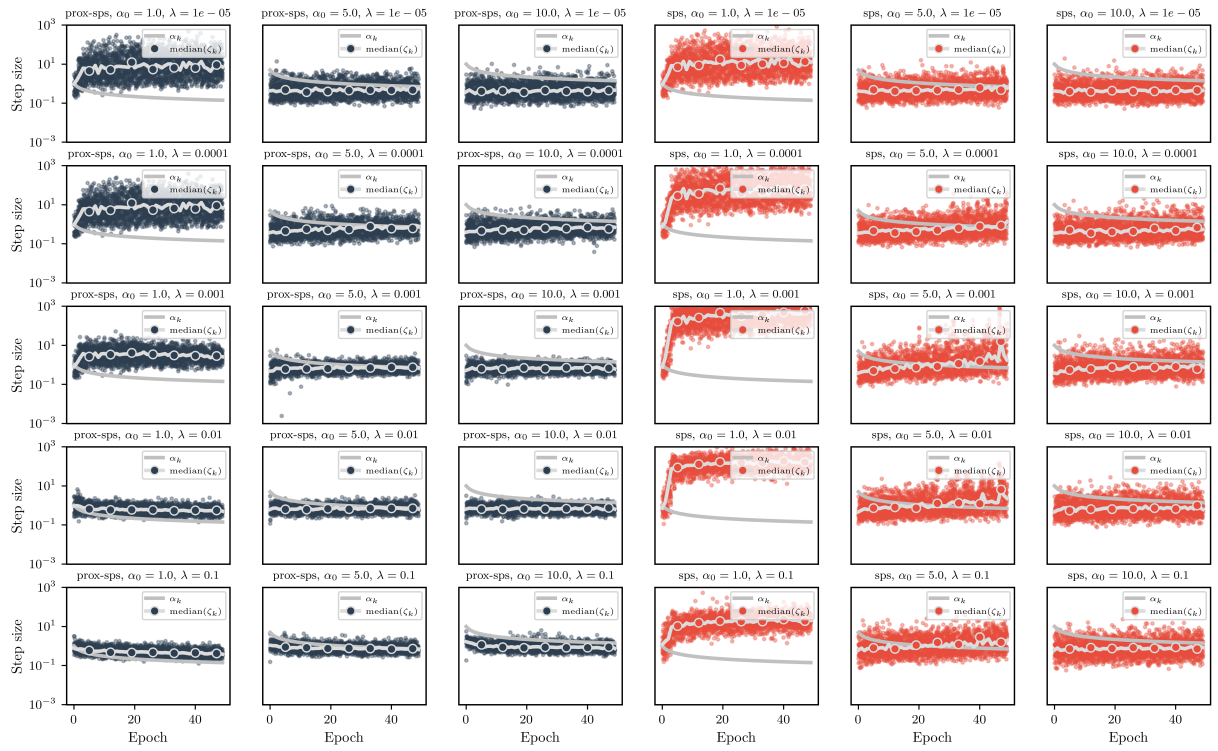


Figure 6: Adaptive step size selection for SPS and ProxSPS. We plot ζ_k (see definition in Section 5.1) as dots for each iteration as well as their median over each epoch. For this plot, we use the results of only one of the ten runs.

5.3 Deep networks for image classification

We train a ResNet56 and ResNet110 model (He et al., 2016) on the CIFAR10 dataset. We use the data loading and preprocessing procedure and network implementation from https://github.com/akamaster/pytorch_resnet_cifar10. We do not use batch normalization. The loss function is the cross-entropy loss of the true image class with respect to the predicted class probabilities, being the output of the ResNet56 network. We add $\frac{\lambda}{2} \|x\|^2$ as regularization term, where x consists of all learnable parameters of the model. The CIFAR10 dataset consist of 60,000 images, each of size 32×32 , from ten different classes. We use the PyTorch split into 50,000 training and 10,000 test examples and use a batch size of 128. For AdamW, we set the weight decay parameter to λ and set all other hyperparameters to its default. We use the AdamW-implementation from <https://github.com/zhenxun-zhuang/AdamW-Scale-free> as it does not – in contrast to the Pytorch implementation – multiply the weight decay parameter with the learning rate, which leads to better comparability to SPS and ProxSPS for identical values of λ . For SPS and ProxSPS we use the sqrt-schedule and $\alpha_0 = 1$. We run each method repeatedly using (the same) three different seeds for the dataset shuffling.

Discussion: For Resnet56, from the bottom plot in Fig. 7, we observe that both SPS and ProxSPS work well with ProxSPS leading to smaller weights. For $\lambda = 5e - 4$, the progress of ProxSPS stagnates after roughly 25 epochs. This can be explained by looking at the adaptive step size term ζ_k in Fig. 9a: as it decays over time we have $\tau_k^+ = \zeta_k \ll \alpha_k$. Since every iteration of ProxSPS shrinks the weights by a factor $\frac{1}{1+\alpha_k\lambda}$, this leads to a bias towards zero. This suggests that we should choose α_k roughly of the order of ζ_k , for example by using the values of ζ_k from the previous epoch.

For the larger model Resnet110 however, SPS does not make progress for a long time because the adaptive step size is very small (see Fig. 8 and Fig. 9b). ProxSPS does not share this issue and performs well after a

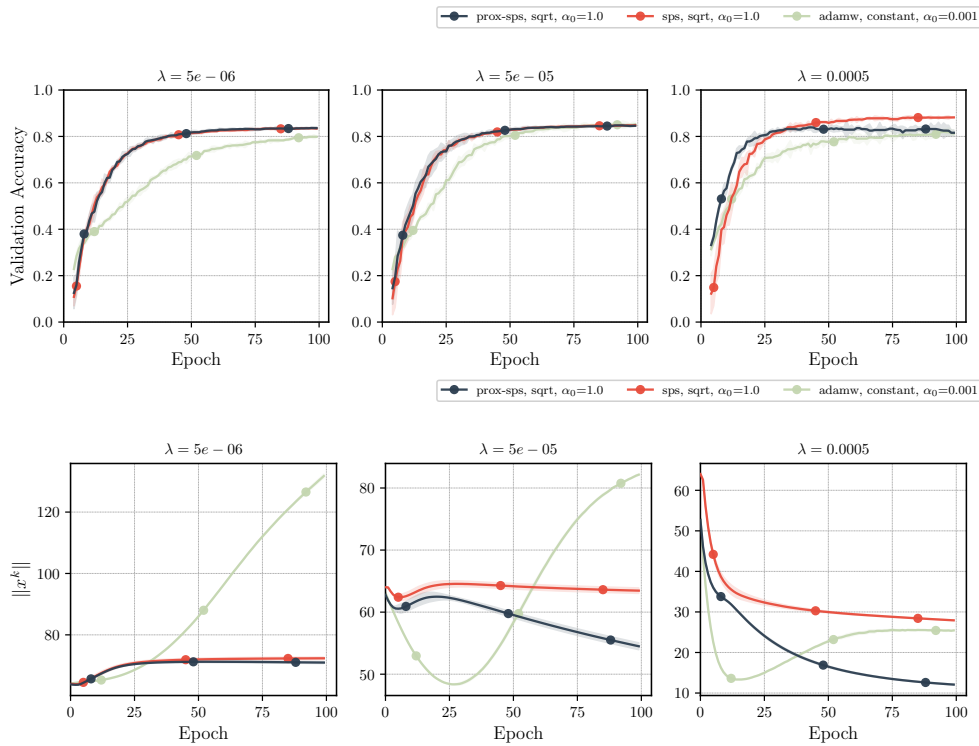


Figure 7: **ResNet56:** (Top): Validation accuracy and model norm for three values of the regularization parameter λ . Validation accuracy is defined as the ratio of correctly labeled images on the validation set (i.e. *Top-1 accuracy*), plotted as five-epoch running median. (Bottom): With $\|x^k\|$ we denote the norm of all learnable parameters at the k -th iteration. Shaded area is two standard deviations over three independent runs.

few initial epochs. For larger values of λ , the training is also considerably faster than for **AdamW**. Generally, we observe that **ProxSPS** (and **SPS** for **Resnet56**) performs well in comparison to **AdamW**. This is achieved without extensive hyperparameter tuning (in particular this suggests that setting $c = 1$ in **SPS_{max}** leads to good results and reduces tuning effort).

6 Conclusion

We proposed and analyzed **ProxSPS**, a proximal version of the stochastic Polyak step size. We arrived at **ProxSPS** by using the framework of stochastic model-based proximal point methods. We then used this framework to argue that the resulting model of **ProxSPS** is a better approximation as compared to the model used by **SPS** when using regularization. Our theoretical results cover a wide range of optimization problems, including convex and nonconvex settings. We performed a series of experiments comparing **ProxSPS**, **SPS**, **SGD** and **AdamW** when using ℓ_2 -regularization. In particular we found that **SPS** can be very hard to tune when using ℓ_2 -regularization, and in contrast, **ProxSPS** performs well for a wide choice of step sizes and regularization parameters. Finally, for our experiments on image classification, we found that **ProxSPS** is competitive to **AdamW**, whereas **SPS** can fail for larger models. At the same time **ProxSPS** produces smaller weights in the trained neural network. Having small weights may help reduce the memory footprint of the resulting network, and even suggests which weights can be pruned.

References

- Hilal Asi and John C. Duchi. Stochastic (approximate) proximal point methods: convergence, optimality, and adaptivity. *SIAM Journal on Optimization*, 29(3):2257–2290, 2019. ISSN 1052-6234. doi: 10.1137/18M1230323.

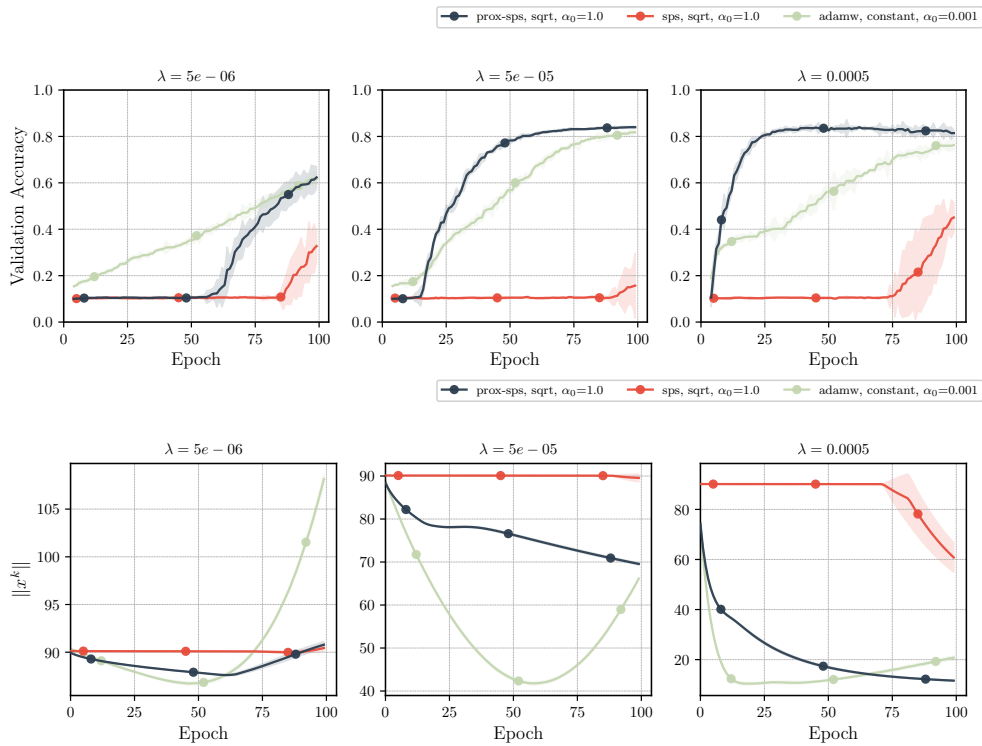


Figure 8: *ResNet110*: Validation accuracy as five-epoch running median (top) and model norm (bottom) for three values of λ . Shaded area is two standard deviations over three independent runs.

Amir Beck. *First-order methods in optimization*, volume 25 of *MOS-SIAM Series on Optimization*. Society for Industrial and Applied Mathematics (SIAM), Philadelphia, 2017. ISBN 978-1-611974-98-0. doi: 10.1137/1.9781611974997.ch1.

Leonard Berrada, Andrew Zisserman, and M. Pawan Kumar. Training neural networks for and by interpolation. June 2019.

D. P. Bertsekas. Stochastic optimization problems with nondifferentiable cost functionals. *Journal of Optimization Theory and Applications*, 12:218–231, 1973. ISSN 0022-3239. doi: 10.1007/BF00934819.

Léon Bottou. Large-scale machine learning with stochastic gradient descent. In *Proceedings of COMPSTAT'2010*, pp. 177–186. Physica-Verlag/Springer, Heidelberg, 2010.

Léon Bottou, Frank E. Curtis, and Jorge Nocedal. Optimization methods for large-scale machine learning. *SIAM Review*, 60(2):223–311, 2018. ISSN 0036-1445. doi: 10.1137/16M1080173.

Frank H. Clarke. *Optimization and nonsmooth analysis*. Canadian Mathematical Society Series of Monographs and Advanced Texts. John Wiley & Sons, Inc., New York, 1983. ISBN 0-471-87504-X. A Wiley-Interscience Publication.

Damek Davis and Dmitriy Drusvyatskiy. Stochastic model-based minimization of weakly convex functions. *SIAM Journal on Optimization*, 29(1):207–239, 2019. ISSN 1052-6234. doi: 10.1137/18M1178244.

D. Drusvyatskiy and C. Paquette. Efficiency of minimizing compositions of convex functions and smooth maps. *Mathematical Programming*, 178(1-2, Ser. A):503–558, 2019. ISSN 0025-5610. doi: 10.1007/s10107-018-1311-3.

Robert Gower, Othmane Sebbouh, and Nicolas Loizou. Sgd for structured nonconvex functions: Learning rates, minibatching and interpolation. In Arindam Banerjee and Kenji Fukumizu (eds.), *Proceedings of The 24th International Conference on Artificial Intelligence and Statistics*, volume 130 of *Proceedings of*

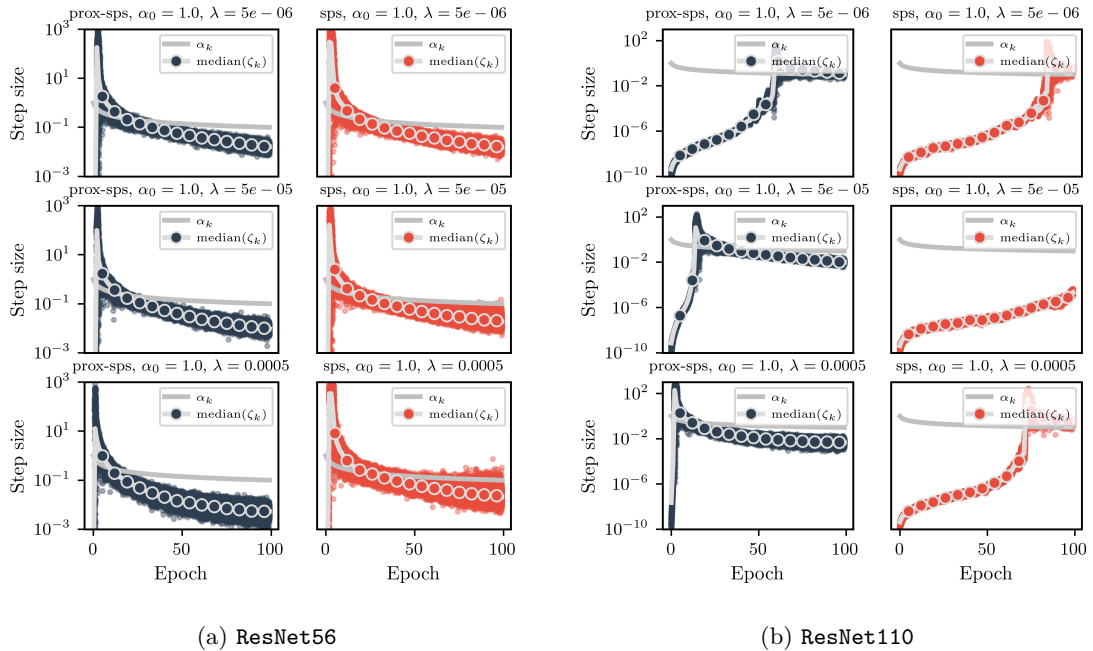


Figure 9: Adaptive step sizes for SPS and ProxSPS. See definition of ζ_k in Section 5.1. For this plot, we use the results of only one of the three runs.

Machine Learning Research, pp. 1315–1323. PMLR, 13–15 Apr 2021. URL <https://proceedings.mlr.press/v130/gower21a.html>.

Elad Hazan and Sham Kakade. Revisiting the polyak step size. May 2019.

Kaiming He, Xiangyu Zhang, Shaoqing Ren, and Jian Sun. Deep residual learning for image recognition. In *2016 IEEE Conference on Computer Vision and Pattern Recognition (CVPR)*, pp. 770–778, 2016. doi: 10.1109/CVPR.2016.90.

Diederik P. Kingma and Jimmy Ba. Adam: A method for stochastic optimization. In Yoshua Bengio and Yann LeCun (eds.), *3rd International Conference on Learning Representations, ICLR 2015, San Diego, CA, USA, May 7-9, 2015, Conference Track Proceedings*, 2015.

Nicolas Loizou, Sharan Vaswani, Issam Hadj Laradji, and Simon Lacoste-Julien. Stochastic polyak step-size for sgd: An adaptive learning rate for fast convergence. In *Proceedings of The 24th International Conference on Artificial Intelligence and Statistics*, volume 130 of *Proceedings of Machine Learning Research*, pp. 1306–1314. PMLR, 13–15 Apr 2021.

Ilya Loshchilov and Frank Hutter. Decoupled weight decay regularization. In *7th International Conference on Learning Representations, ICLR 2019, New Orleans, LA, USA, May 6-9, 2019*. OpenReview.net, 2019. URL <https://openreview.net/forum?id=Bkg6RiCqY7>.

Antonio Orvieto, Simon Lacoste-Julien, and Nicolas Loizou. Dynamics of sgd with stochastic polyak stepsizes: Truly adaptive variants and convergence to exact solution. May 2022.

Alasdair Paren, Leonard Berrada, Rudra P. K. Poudel, and M. Pawan Kumar. A stochastic bundle method for interpolation. *Journal of Machine Learning Research*, 23(15):1–57, 2022. URL <http://jmlr.org/papers/v23/20-1248.html>.

Adam Paszke, Sam Gross, Francisco Massa, Adam Lerer, James Bradbury, Gregory Chanan, Trevor Killeen, Zeming Lin, Natalia Gimelshein, Luca Antiga, Alban Desmaison, Andreas Kopf,

Edward Yang, Zachary DeVito, Martin Raison, Alykhan Tejani, Sasank Chilamkurthy, Benoit Steiner, Lu Fang, Junjie Bai, and Soumith Chintala. Pytorch: An imperative style, high-performance deep learning library. In *Advances in Neural Information Processing Systems 32*, pp. 8024–8035. Curran Associates, Inc., 2019. URL <http://papers.neurips.cc/paper/9015-pytorch-an-imperative-style-high-performance-deep-learning-library.pdf>.

Boris T. Polyak. *Introduction to optimization*. Translations Series in Mathematics and Engineering. Optimization Software, Inc., Publications Division, New York, 1987. ISBN 0-911575-14-6. Translated from the Russian, With a foreword by Dimitri P. Bertsekas.

Mariana Prazeres and Adam M. Oberman. Stochastic gradient descent with Polyak’s learning rate. *Journal of Scientific Computing*, 89(1):Paper No. 25, 16, 2021. ISSN 0885-7474. doi: 10.1007/s10915-021-01628-3.

Herbert Robbins and Sutton Monro. A stochastic approximation method. *Ann. Math. Statistics*, 22:400–407, 1951. ISSN 0003-4851. doi: 10.1214/aoms/1177729586.

R. Tyrrell Rockafellar and Roger J.-B. Wets. *Variational analysis*, volume 317 of *Grundlehren der mathematischen Wissenschaften [Fundamental Principles of Mathematical Sciences]*. Springer-Verlag, Berlin, 1998. ISBN 3-540-62772-3. doi: 10.1007/978-3-642-02431-3.

Nathan Srebro, Jason Rennie, and Tommi Jaakkola. Maximum-margin matrix factorization. In L. Saul, Y. Weiss, and L. Bottou (eds.), *Advances in Neural Information Processing Systems*, volume 17. MIT Press, 2004. URL <https://proceedings.neurips.cc/paper/2004/file/e0688d13958a19e087e123148555e4b4-Paper.pdf>.

Zhenxun Zhuang, Mingrui Liu, Ashok Cutkosky, and Francesco Orabona. Understanding adamw through proximal methods and scale-freeness. January 2022.

Contents

1	Introduction	1
1.1	Background and Contributions	2
2	Preliminaries	3
2.1	Notation	3
2.2	General assumptions	3
2.3	Convex analysis	3
3	The unregularized case	4
3.1	A model-based view point	4
4	The regularized case	5
4.1	The special case of ℓ_2 -regularization	6
4.2	Comparing the model of SPS and ProxSPS	7
4.3	Convergence analysis	7
4.3.1	Globally bounded subgradients	8
4.3.2	Lipschitz smoothness	9
4.3.3	Comparison to existing theory	11
5	Numerical experiments	12
5.1	General parameter setting	12
5.2	Regularized matrix factorization	12
5.3	Deep networks for image classification	15
6	Conclusion	16
A	Missing Proofs	21
A.1	Proofs of model-based update formula	21
A.2	Proof of Theorem 7	23
A.3	Proof of Theorem 8	24
B	Auxiliary Lemmas	26
C	Model equivalence for SGD	27
D	Additional information on numerical experiments	27
D.1	Matrix Factorization	27
D.2	Plots for <code>matrix-fac2</code>	28
D.3	Interpolation constant	29

A Missing Proofs

A.1 Proofs of model-based update formula

Lemma 9. For $\lambda \geq 0$, let $\varphi(x) = \frac{\lambda}{2}\|x\|^2$ and let $g \in \partial f(x; s)$ and $C(s) \leq \inf_{z \in \mathbb{R}^n} f(z; s)$ hold for all $s \in \mathcal{S}$. For

$$\psi_x(y; s) = f_x(y; s) + \varphi(y), \quad f_x(y; s) = \max\{f(x; s) + \langle g, y - x \rangle, C(s)\},$$

consider the update

$$x^{k+1} = \arg \min_{x \in \mathbb{R}^n} \psi_{x^k}(x; S_k) + \frac{1}{2\alpha_k} \|x - x^k\|^2. \quad (29)$$

Denote $C_k := C(S_k)$ and let $g_k \in \partial f(x^k; S_k)$. Define

$$\tau_k^+ := \begin{cases} 0 & \text{if } g_k = 0, \\ \min \left\{ \alpha_k, \left(\frac{(1+\alpha_k\lambda)(f(x^k; S_k) - C_k) - \alpha_k\lambda\langle g_k, x^k \rangle}{\|g_k\|^2} \right)_+ \right\} & \text{else.} \end{cases}$$

Then, we have

$$x^{k+1} = \frac{1}{1+\alpha_k\lambda} x^k - \frac{\tau_k^+}{1+\alpha_k\lambda} g_k = \frac{1}{1+\alpha_k\lambda} \left(x^k - \tau_k^+ g_k \right) = \text{prox}_{\alpha_k\varphi}(x^k - \tau_k^+ g_k). \quad (30)$$

Define $\tau_k := 0$ if $g_k = 0$ and $\tau_k := \min \left\{ \alpha_k, \frac{(1+\alpha_k\lambda)(f(x^k; S_k) - C_k) - \alpha_k\lambda\langle g_k, x^k \rangle}{\|g_k\|^2} \right\}$ else. Then, it holds $\tau_k \leq \tau_k^+$ and

$$\psi_{x^k}(x^{k+1}; S_k) = f(x^k; S_k) - \frac{\alpha_k\lambda}{1+\alpha_k\lambda} \langle g_k, x^k \rangle - \frac{\tau_k}{1+\alpha_k\lambda} \|g_k\|^2 + \varphi(x^{k+1}). \quad (31)$$

Proof. Note that $\max\{f(x^k; S_k) + \langle g_k, y - x^k \rangle, C_k\}$ is convex as a function of y . The update is therefore unique. First, if $g_k = 0$, then clearly $x^{k+1} = \text{prox}_{\alpha_k\varphi}(x^k) = \frac{1}{1+\alpha_k\lambda} x^k$ and (31) holds true. Now, let $g_k \neq 0$. The solution of (29) is either in $\{y | f(x^k; S_k) + \langle g_k, y - x^k \rangle < C_k\}$, or in $\{y | f(x^k; S_k) + \langle g_k, y - x^k \rangle > C_k\}$ or in $\{y | f(x^k; S_k) + \langle g_k, y - x^k \rangle = C_k\}$. We therefore solve three problems:

(P1) Solve

$$y^+ = \arg \min_y C_k + \frac{\lambda}{2} \|y\|^2 + \frac{1}{2\alpha_k} \|y - x^k\|^2.$$

Clearly, the solution is $y^+ = \frac{1}{1+\alpha_k\lambda} x^k$. This y^+ solves (29) if $f(x^k; S_k) + \langle g_k, y^+ - x^k \rangle < C_k$.

(P2) Solve

$$y^+ = \arg \min_y f(x^k; S_k) + \langle g_k, y - x^k \rangle + \frac{\lambda}{2} \|y\|^2 + \frac{1}{2\alpha_k} \|y - x^k\|^2.$$

The optimality condition is $0 = \alpha_k g_k + \alpha_k \lambda y^+ + y^+ - x^k$. Thus, the solution is $y^+ = \frac{1}{1+\alpha_k\lambda} (x^k - \alpha_k g_k)$. This y^+ solves (29) if $f(x^k; S_k) + \langle g_k, y^+ - x^k \rangle > C_k$.

(P3) Solve

$$y^+ = \arg \min_y \frac{\lambda}{2} \|y\|^2 + \frac{1}{2\alpha_k} \|y - x^k\|^2, \quad \text{s.t. } f(x^k; S_k) + \langle g_k, y - x^k \rangle = C_k.$$

The KKT conditions are given by

$$\begin{aligned} \alpha_k \lambda y + y - x^k + \mu g_k &= 0, \\ f(x^k; S_k) + \langle g_k, y - x^k \rangle &= C_k. \end{aligned}$$

Taking the inner product of the first equation with g_k , we get

$$(1 + \alpha_k \lambda) \langle g_k, y \rangle - \langle g_k, x^k \rangle + \mu \|g_k\|^2 = 0.$$

From the second KKT condition we have $\langle g_k, y \rangle = C_k - f(x^k; S_k) + \langle g_k, x^k \rangle$, hence

$$(1 + \alpha_k \lambda)(C_k - f(x^k; S_k) + \langle g_k, x^k \rangle) - \langle g_k, x^k \rangle + \mu \|g_k\|^2 = 0.$$

Solving for μ gives $\mu = \frac{(1 + \alpha_k \lambda)(f(x^k; S_k) - C_k) - \alpha_k \lambda \langle g_k, x^k \rangle}{\|g_k\|^2}$. From the first KKT condition, we obtain

$$y^+ = \frac{1}{1 + \alpha_k \lambda} (x^k - \mu g_k) = \frac{1}{1 + \alpha_k \lambda} \left(x^k - \frac{(1 + \alpha_k \lambda)(f(x^k; S_k) - C_k) - \alpha_k \lambda \langle g_k, x^k \rangle}{\|g_k\|^2} g_k \right).$$

This y^+ solves (29) if neither (P1) nor (P2) provided a solution.

For all three cases, the solution takes the form $y^+ = \frac{1}{1 + \alpha_k \lambda} [x^k - t g_k] =: y(t)$. As $\|g_k\|^2 > 0$, the term $f(x^k; S_k) + \langle g_k, y(t) - x^k \rangle$ is strictly monotonically decreasing in t . We know $f(x^k; S_k) + \langle g_k, y(t) - x^k \rangle = C_k$ for $t = \mu$ (from (P3)). Hence, $f(x^k; S_k) + \langle g_k, y(t) - x^k \rangle < C_k (> C_k)$ if and only if $t > \mu$ ($t < \mu$).

We conclude:

- If $f(x^k; S_k) + \langle g_k, y(0) - x^k \rangle < C_k$, then the solution to (P1) is the solution to (29). This condition is equivalent to $\mu < 0$.
- If $f(x^k; S_k) + \langle g_k, y(\alpha_k) - x^k \rangle > C_k$, then the solution to (P2) is the solution to (29). This condition is equivalent to $\alpha_k < \mu$.
- If neither $0 > \mu$ nor $\alpha_k < \mu$ hold, i.e. if $\mu \in [0, \alpha_k]$, then the solution to (29) comes from (P3) and hence is given by $y(\mu)$.

Altogether, we get that $x^{k+1} = \frac{1}{1 + \alpha_k \lambda} [x^k - \tau_k^+ g_k]$ with $\tau_k^+ = \min\{\alpha_k, (\mu)_+\}$.

Now, we prove (31). Note that if $g_k \neq 0$, then $\tau_k = \min\{\alpha_k, \mu\}$ with μ defined as in (P3). In the case of (P1), we have $\psi_{x^k}(x^{k+1}; S_k) = C_k + \varphi(x^{k+1})$. Moreover, it holds $\mu < 0$ and as $\alpha_k > 0$ we have $\tau_k = \mu$. Plugging $\tau_k = \mu$ into the right hand-side of (31), we obtain $C_k + \varphi(x^{k+1})$.

In the case of (P2) or (P3), we have $C_k \leq f(x^k; S_k) + \langle g_k, x^{k+1} - x^k \rangle$. Due to $f(x^k; S_k) + \langle g_k, y(t) - x^k \rangle = f(x^k; S_k) - \frac{1}{1 + \alpha_k \lambda} \langle g_k, x^k \rangle + \frac{t}{1 + \alpha_k \lambda} \|g_k\|^2$, we obtain (31) as $x^{k+1} = y(\alpha_k)$ and $\mu > \alpha_k$ in the case of (P2) and $x^{k+1} = y(\mu)$ and $\mu \leq \alpha_k$ in the case of (P3). \square

Lemma 10. Consider the model $f_x(y; s) := \max\{f(x; s) + \langle g, y - x \rangle, C(s)\}$ where $g \in \partial f(x; s)$ and $C(s) \leq \inf_{z \in \mathbb{R}^n} f(z; s)$ holds for all $s \in \mathcal{S}$. Then, update (5) is given as

$$x^{k+1} = x^k - \gamma_k g_k, \quad \gamma_k = \begin{cases} 0 & \text{if } g_k = 0, \\ \min\left\{\alpha_k, \frac{f(x^k; S^k) - C(S_k)}{\|g_k\|^2}\right\} & \text{else.} \end{cases}$$

where $g_k \in \partial f(x^k; S_k)$. Moreover, it holds

$$f_{x^k}(x^{k+1}; S_k) = \max\{C(S_k), f(x^k; S_k) - \alpha_k \|g_k\|^2\}, \quad (32)$$

and therefore $f_{x^k}(x^{k+1}; S_k) = f(x^k; S_k) - \gamma_k \|g_k\|^2$.

Proof. We apply Lemma 9 with $\lambda = 0$. As $f(x^k; S_k) \geq C(S_k)$, we have that $\tau_k^+ = \tau_k = \gamma_k$. \square

A.2 Proof of Theorem 7

From now on, denote with \mathcal{F}_k the filtration that is generated by the history of all S_j for $j = 0, \dots, k - 1$.

Proof of Theorem 7. In the proof, we will denote $g_k = \nabla f(x^k; S_k)$. We apply Lemma 6, (16) with $x = x^*$. Due to Lemma 2 (ii) and convexity of $f(\cdot; s)$ it holds

$$\psi_{x^k}(x^*; S_k) \leq f(x^*; S_k) + \varphi(x^*).$$

Together with (17), we have

$$(1 + \alpha_k \lambda) \|x^{k+1} - x^*\|^2 \leq \|x^k - x^*\|^2 - \|x^{k+1} - x^k\|^2 + 2\alpha_k [\varphi(x^*) - \varphi(x^{k+1})] + 2\alpha_k [f(x^*; S_k) - f(x^k; S_k) - \langle g_k, x^{k+1} - x^k \rangle]. \quad (33)$$

Smoothness of f yields

$$-f(x^k) \leq -f(x^{k+1}) + \langle \nabla f(x^k), x^{k+1} - x^k \rangle + \frac{L}{2} \|x^{k+1} - x^k\|^2.$$

Consequently,

$$\begin{aligned} -\langle g_k, x^{k+1} - x^k \rangle &= f(x^k) - f(x^k) - \langle g_k, x^{k+1} - x^k \rangle \\ &\leq f(x^k) - f(x^{k+1}) + \langle \nabla f(x^k) - g_k, x^{k+1} - x^k \rangle + \frac{L}{2} \|x^{k+1} - x^k\|^2 \\ &\leq f(x^k) - f(x^{k+1}) + \frac{\theta \alpha_k}{2} \|\nabla f(x^k) - g_k\|^2 + \frac{1}{2\theta \alpha_k} \|x^{k+1} - x^k\|^2 + \frac{L}{2} \|x^{k+1} - x^k\|^2. \end{aligned}$$

for any $\theta > 0$, where we used Young's inequality in the last step. Plugging into (33) gives

$$(1 + \alpha_k \lambda) \|x^{k+1} - x^*\|^2 \leq \|x^k - x^*\|^2 + [\alpha_k L + \frac{1}{\theta} - 1] \|x^{k+1} - x^k\|^2 + 2\alpha_k [\varphi(x^*) - \varphi(x^{k+1})] + 2\alpha_k [f(x^*; S_k) - f(x^k; S_k) + f(x^k) - f(x^{k+1})] + \theta \alpha_k^2 \|\nabla f(x^k) - g_k\|^2.$$

Applying conditional expectation, we have $\mathbb{E}[f(x^*; S_k) | \mathcal{F}_k] = f(x^*)$ and

$$\mathbb{E}[-f(x^k; S_k) + f(x^k) | \mathcal{F}_k] = 0, \quad \mathbb{E}[\|\nabla f(x^k) - g_k\|^2 | \mathcal{F}_k] \leq \beta.$$

Moreover, by assumption, $\alpha_k L + \frac{1}{\theta} - 1 \leq 0$. Altogether, applying total expectation yields

$$(1 + \alpha_k \lambda) \mathbb{E}\|x^{k+1} - x^*\|^2 \leq \mathbb{E}\|x^k - x^*\|^2 + 2\alpha_k \mathbb{E}[\psi(x^*) - \psi(x^{k+1})] + \theta \beta \alpha_k^2$$

which proves (20).

Proof of a): let $\alpha_k = \frac{1}{\lambda(k+k_0)}$. Denote $\Delta_k := \mathbb{E}\|x^k - x^*\|^2$. Rearranging and summing (20), we have

$$\sum_{k=0}^{K-1} \mathbb{E}[\psi(x^{k+1}) - \psi(x^*)] \leq \sum_{k=0}^{K-1} \left[\frac{1}{2\alpha_k} \Delta_k - \frac{1+\alpha_k \lambda}{2\alpha_k} \Delta_{k+1} + \frac{\theta \beta \alpha_k}{2} \right].$$

Plugging in α_k , we have $\frac{1+\alpha_k \lambda}{2\alpha_k} = \frac{\lambda(k+k_0)}{2} + \frac{\lambda}{2}$ and thus

$$\sum_{k=0}^{K-1} \mathbb{E}[\psi(x^{k+1}) - \psi(x^*)] \leq \sum_{k=0}^{K-1} \left[\frac{\lambda(k+k_0)}{2} \Delta_k - \frac{\lambda(k+1+k_0)}{2} \Delta_{k+1} \right] + \frac{\theta \beta}{2} \sum_{k=0}^{K-1} \frac{1}{\lambda(k+k_0)}.$$

Dividing by K and using convexity of ψ ⁹, we have

$$\mathbb{E}\left[\psi\left(\frac{1}{K} \sum_{k=0}^{K-1} x^{k+1}\right) - \psi(x^*)\right] \leq \frac{\lambda k_0}{2K} \|x^0 - x^*\|^2 + \frac{\theta \beta}{2\lambda K} \sum_{k=0}^{K-1} \frac{1}{k+k_0}.$$

⁹By assumption f is convex and therefore ψ is convex.

Finally, as $k_0 \geq 1$, we estimate $\sum_{k=0}^{K-1} \frac{1}{k+k_0} \leq \sum_{k=0}^{K-1} \frac{1}{k+1} \leq 1 + \ln K$ by [Lemma 13](#) and obtain (21).

Proof of b): Similar to the proof above, we rearrange and sum (20) from $k = 0, \dots, K-1$, and obtain

$$\sum_{k=0}^{K-1} \alpha_k \mathbb{E}[\psi(x^{k+1}) - \psi(x^*)] \leq \frac{\|x^0 - x^*\|^2}{2} + \frac{\theta\beta \sum_{k=0}^{K-1} \alpha_k^2}{2}.$$

We divide by $\sum_{k=0}^{K-1} \alpha_k$ and use convexity of ψ in order to obtain the left-hand side of (22). Moreover, by [Lemma 13](#) we have

$$\sum_{k=0}^{K-1} \alpha_k \geq 2\alpha(\sqrt{K+1} - 1), \quad \sum_{k=0}^{K-1} \alpha_k^2 \leq \alpha^2(1 + \ln K).$$

Plugging in the above estimates, gives

$$\mathbb{E}\left[\psi\left(\frac{1}{\sum_{k=0}^{K-1} \alpha_k} \sum_{k=0}^{K-1} \alpha_k x^{k+1}\right) - \psi(x^*)\right] \leq \frac{\|x^0 - x^*\|^2}{4\alpha(\sqrt{K+1} - 1)} + \frac{\theta\beta\alpha(1 + \ln K)}{4(\sqrt{K+1} - 1)}.$$

Proof of c): If f is μ -strongly-convex, then ψ is $(\lambda + \mu)$ -strongly convex and

$$\psi(x^*) - \psi(x^{k+1}) \leq -\frac{\mu+\lambda}{2} \|x^{k+1} - x^*\|^2.$$

From (20), with $\alpha_k = \alpha$, we get

$$(1 + \alpha(\mu + 2\lambda))\mathbb{E}\|x^{k+1} - x^*\|^2 \leq \mathbb{E}\|x^k - x^*\|^2 + \theta\beta\alpha^2.$$

Doing a recursion of the above from $k = 0, \dots, K-1$ gives

$$\mathbb{E}\|x^K - x^*\|^2 \leq (1 + \alpha(\mu + 2\lambda))^{-K} \|x^0 - x^*\|^2 + \theta\beta\alpha^2 \sum_{k=1}^K (1 + \alpha(\mu + 2\lambda))^{-k}$$

Using the geometric series, $\sum_{k=1}^K (1 + \alpha(\mu + 2\lambda))^{-k} \leq \frac{1 + \alpha(\mu + 2\lambda)}{\alpha(\mu + 2\lambda)} - 1 = \frac{1}{\alpha(\mu + 2\lambda)}$, and thus

$$\mathbb{E}\|x^K - x^*\|^2 \leq (1 + \alpha(\mu + 2\lambda))^{-K} \|x^0 - x^*\|^2 + \frac{\theta\beta\alpha}{\mu + 2\lambda}.$$

□

A.3 Proof of [Theorem 8](#)

Proof of [Theorem 8](#). In the proof, we will denote $g_k = \nabla f(x^k; S_k)$. By assumption f is ρ -weakly convex and hence ψ is $(\rho - \lambda)$ -weakly convex if $\rho > \lambda$ and convex if $\rho \leq \lambda$. Hence, $\hat{x}^k := \text{prox}_{\eta\psi}(x^k)$ is well-defined for $\eta < 1/(\rho - \lambda)$ if $\rho > \lambda$ and for any $\eta > 0$ else. Note that \hat{x}^k is \mathcal{F}_k -measurable. We apply [Lemma 6](#), (16) with $x = \hat{x}^k$. Due to [Lemma 2 \(ii\)](#) it holds

$$\psi_{x^k}(\hat{x}^k; S_k) = f_{x^k}(\hat{x}^k; S_k) + \varphi(\hat{x}^k) \leq f(\hat{x}^k; S_k) + \frac{\rho_{S_k}}{2} \|\hat{x}^k - x^k\|^2 + \varphi(\hat{x}^k).$$

Together with (17), this gives

$$\begin{aligned} (1 + \alpha_k \lambda) \|x^{k+1} - \hat{x}^k\|^2 &\leq (1 + \alpha_k \rho_{S_k}) \|x^k - \hat{x}^k\|^2 - \|x^{k+1} - x^k\|^2 \\ &\quad + 2\alpha_k (\varphi(\hat{x}^k) - \varphi(x^{k+1}) + f(\hat{x}^k; S_k) - f(x^k; S_k) - \langle g_k, x^{k+1} - x^k \rangle) \end{aligned}$$

Analogous to the proof of [Theorem 7](#), due to Lipschitz smoothness, for all $\theta > 0$ we have

$$\begin{aligned} -f(x^k; S_k) - \langle g_k, x^{k+1} - x^k \rangle &\leq -f(x^k; S_k) + f(x^k) \\ &\quad - f(x^{k+1}) + \frac{\theta\alpha_k}{2} \|\nabla f(x^k) - g_k\|^2 + \left[\frac{1}{2\theta\alpha_k} + \frac{L}{2} \right] \|x^{k+1} - x^k\|^2. \end{aligned}$$

Plugging in gives

$$\begin{aligned} (1 + \alpha_k \lambda) \|x^{k+1} - \hat{x}^k\|^2 &\leq (1 + \alpha_k \rho_{S_k}) \|x^k - \hat{x}^k\|^2 + 2\alpha_k (\varphi(\hat{x}^k) - \varphi(x^{k+1})) \\ &\quad + 2\alpha_k (f(\hat{x}^k; S_k) - f(x^k; S_k) + f(x^k) - f(x^{k+1}) + \frac{\theta \alpha_k}{2} \|\nabla f(x^k) - g_k\|^2) \\ &\quad + [\frac{1}{\theta} + \alpha_k L - 1] \|x^{k+1} - x^k\|^2. \end{aligned}$$

It holds $\mathbb{E}[f(\hat{x}^k; S_k) - f(x^k; S_k) | \mathcal{F}_k] = f(\hat{x}^k) - f(x^k)$ and $\mathbb{E}[\psi(\hat{x}^k) | \mathcal{F}_k] = \psi(\hat{x}^k)$. By [Assumption 4](#), we have $\mathbb{E}[\|g_k - \nabla f(x^k)\|^2 | \mathcal{F}_k] \leq \beta$. Altogether, taking conditional expectation yields

$$\begin{aligned} (1 + \alpha_k \lambda) \mathbb{E}[\|x^{k+1} - \hat{x}^k\|^2 | \mathcal{F}_k] &\leq (1 + \alpha_k \rho) \|x^k - \hat{x}^k\|^2 + 2\alpha_k \mathbb{E}[\psi(\hat{x}^k) - \psi(x^{k+1}) | \mathcal{F}_k] \\ &\quad + \alpha_k^2 \theta \beta + [\frac{1}{\theta} + \alpha_k L - 1] \mathbb{E}[\|x^{k+1} - x^k\|^2 | \mathcal{F}_k]. \end{aligned}$$

Next, the definition of the proximal operator implies that almost surely

$$\psi(\hat{x}^k) + \frac{1}{2\eta} \|\hat{x}^k - x^k\|^2 \leq \psi(x^{k+1}) + \frac{1}{2\eta} \|x^{k+1} - x^k\|^2,$$

and hence

$$\mathbb{E}[\psi(\hat{x}^k) - \psi(x^{k+1}) | \mathcal{F}_k] \leq \mathbb{E}\left[\frac{1}{2\eta} \|x^{k+1} - x^k\|^2 - \frac{1}{2\eta} \|\hat{x}^k - x^k\|^2 | \mathcal{F}_k\right].$$

Altogether, we have

$$\begin{aligned} (1 + \alpha_k \lambda) \mathbb{E}[\|x^{k+1} - \hat{x}^k\|^2 | \mathcal{F}_k] &\leq (1 + \alpha_k(\rho - \eta^{-1})) \|x^k - \hat{x}^k\|^2 \\ &\quad + \alpha_k^2 \theta \beta + [\frac{1}{\theta} + \alpha_k L + \alpha_k \eta^{-1} - 1] \mathbb{E}[\|x^{k+1} - x^k\|^2 | \mathcal{F}_k]. \end{aligned}$$

From assumption [\(24\)](#), we can drop the last term. Now, we aim for a recursion in $\text{env}_{\psi}^{\eta}(x^k)$. Using that

$$\frac{1 + \alpha_k(\rho - \eta^{-1})}{1 + \alpha_k \lambda} = \frac{1 + \alpha_k \lambda - \alpha_k \lambda + \alpha_k(\rho - \eta^{-1})}{1 + \alpha_k \lambda} = 1 + \frac{\alpha_k(\rho - \eta^{-1} - \lambda)}{1 + \alpha_k \lambda} \leq 1 + \alpha_k(\rho - \eta^{-1} - \lambda),$$

we get

$$\begin{aligned} \mathbb{E}[\text{env}_{\psi}^{\eta}(x^{k+1}) | \mathcal{F}_k] &\leq \mathbb{E}[\psi(\hat{x}^k) + \frac{1}{2\eta} \|x^{k+1} - \hat{x}^k\|^2 | \mathcal{F}_k] \\ &\leq \underbrace{\psi(\hat{x}^k) + \frac{1}{2\eta} \|x^k - \hat{x}^k\|^2}_{=\text{env}_{\psi}^{\eta}(x^k)} + \frac{1}{2\eta} [\alpha_k(\rho - \eta^{-1} - \lambda)] \|x^k - \hat{x}^k\|^2 + \frac{\alpha_k^2}{2\eta} \theta \beta. \end{aligned}$$

Now using $\|x^k - \hat{x}^k\| = \eta \|\nabla \text{env}_{\psi}^{\eta}(x^k)\|$ we conclude

$$\mathbb{E}[\text{env}_{\psi}^{\eta}(x^{k+1}) | \mathcal{F}_k] \leq \text{env}_{\psi}^{\eta}(x^k) + \frac{\eta}{2} [\alpha_k(\rho - \eta^{-1} - \lambda)] \|\nabla \text{env}_{\psi}^{\eta}(x^k)\|^2 + \frac{\alpha_k^2}{2\eta} \theta \beta.$$

Due to [\(24\)](#), we have $\eta^{-1} + \lambda - \rho > 0$. Taking expectation and unfolding the recursion by summing over $k = 0, \dots, K-1$, we get

$$\sum_{k=0}^{K-1} \frac{\alpha_k}{2} (1 - \eta(\rho - \lambda)) \mathbb{E}[\|\nabla \text{env}_{\psi}^{\eta}(x^k)\|^2] \leq \text{env}_{\psi}^{\eta}(x^0) - \mathbb{E}[\text{env}_{\psi}^{\eta}(x^K)] + \sum_{k=0}^{K-1} \frac{\alpha_k^2}{2\eta} \theta \beta.$$

Now using that $\text{env}_{\psi}^{\eta}(x^K) \geq \inf \psi$ almost surely, we finally get

$$\sum_{k=0}^{K-1} \alpha_k \mathbb{E}[\|\nabla \text{env}_{\psi}^{\eta}(x^k)\|^2] \leq \frac{2(\text{env}_{\psi}^{\eta}(x^0) - \inf \psi)}{1 - \eta(\rho - \lambda)} + \frac{\beta \theta}{\eta(1 - \eta(\rho - \lambda))} \sum_{k=0}^{K-1} \alpha_k^2, \quad (34)$$

which proves (25). Now choose $\alpha_k = \frac{\alpha}{\sqrt{k+1}}$ and divide (34) by $\sum_{k=0}^{K-1} \alpha_k$. Using Lemma 13 for $\sum_{k=0}^{K-1} \alpha_k$ and $\sum_{k=0}^{K-1} \alpha_k^2$, we have

$$\min_{k=0, \dots, K-1} \mathbb{E} \|\nabla \text{env}_\psi^\eta(x^k)\|^2 \leq \frac{\text{env}_\psi^\eta(x^0) - \inf \psi}{\alpha(1 - \eta(\rho - \lambda))(\sqrt{K+1} - 1)} + \frac{\beta\theta}{2\eta(1 - \eta(\rho - \lambda))} \frac{\alpha(1 + \ln K)}{(\sqrt{K+1} - 1)}.$$

Choosing $\alpha_k = \frac{\alpha}{\sqrt{K}}$ instead, we can identify the left-hand-side of (34) as $\alpha\sqrt{K}\mathbb{E} \|\nabla \text{env}_\psi^\eta(x_\sim^K)\|^2$. Dividing by $\alpha\sqrt{K}$ and using $\sum_{k=0}^{K-1} \alpha_k^2 = \alpha^2$, we obtain

$$\mathbb{E} \|\nabla \text{env}_\psi^\eta(x_\sim^K)\|^2 \leq \frac{2(\text{env}_\psi^\eta(x^0) - \inf \psi)}{\alpha(1 - \eta(\rho - \lambda))\sqrt{K}} + \frac{\beta\theta}{\eta(1 - \eta(\rho - \lambda))} \frac{\alpha}{\sqrt{K}}.$$

□

B Auxiliary Lemmas

Lemma 11 (Thm. 4.5 in (Drusvyatskiy & Paquette, 2019)). *Let f be L -smooth and φ be proper, closed, convex. For $\eta > 0$, define $\mathcal{G}_\eta(x) := \eta^{-1}(x - \text{prox}_{\eta\varphi}(x - \eta\nabla f(x)))$. It holds*

$$\frac{1}{4} \|\nabla \text{env}_\psi^{1/(2L)}(x)\| \leq \|\mathcal{G}_{1/L}(x)\| \leq \frac{3}{2}(1 + \frac{1}{\sqrt{2}}) \|\nabla \text{env}_\psi^{1/(2L)}(x)\| \quad \forall x \in \mathbb{R}^n.$$

Lemma 12. *Let $c \in \mathbb{R}, a, x^0 \in \mathbb{R}^n$ and $\beta > 0$ and let $\varphi : \mathbb{R}^n \rightarrow \mathbb{R} \cup \{\infty\}$ be proper, closed, convex. The solution to*

$$y^+ = \arg \min_{y \in \mathbb{R}^n} (c + \langle a, y \rangle)_+ + \varphi(y) + \frac{1}{2\beta} \|y - x^0\|^2 \quad (35)$$

is given by

$$y^+ = \begin{cases} \text{prox}_{\beta\varphi}(x^0 - \beta a), & \text{if } c + \langle a, \text{prox}_{\beta\varphi}(x^0 - \beta a) \rangle > 0, \\ \text{prox}_{\beta\varphi}(x^0), & \text{if } c + \langle a, \text{prox}_{\beta\varphi}(x^0) \rangle < 0, \\ \text{prox}_{\beta\varphi}(x^0 - \beta u a) & \text{else, for } u \in [0, 1] \text{ such that } c + \langle a, \text{prox}_{\beta\varphi}(x^0 - \beta u a) \rangle = 0. \end{cases} \quad (36)$$

Remark 3. *The first two conditions can not hold simultaneously due to uniqueness of the solution. If neither of the conditions of the first two cases are satisfied, we have to find the root of $u \mapsto c + \langle a, \text{prox}_{\beta\varphi}(x^0 - \beta u a) \rangle$ for $u \in [0, 1]$. Due to strong convexity of the objective in (35), we know that there exists a root and hence y^+ can be found efficiently with bisection.*

Proof. The objective of (35) is strongly convex and hence there exists a unique solution. Due to (Beck, 2017, Thm. 3.63), y is the solution to (35) if and only if it satisfies first-order optimality, i.e.

$$\exists u \in \partial(\cdot)_+(c + \langle a, y \rangle) : 0 \in ua + \partial\varphi(y) + \frac{1}{\beta}(y - x^0). \quad (37)$$

Now, as $y = \text{prox}_{\beta\varphi}(z) \iff 0 \in \partial\varphi(y) + \frac{1}{\beta}(y - z)$, it holds

$$\begin{aligned} (37) &\iff \exists u \in \partial(\cdot)_+(c + \langle a, y \rangle) : 0 \in \partial\varphi(y) + \frac{1}{\beta}(y - (x^0 - \beta u a)) \\ &\iff \exists u \in \partial(\cdot)_+(c + \langle a, y \rangle) : y = \text{prox}_{\beta\varphi}(x^0 - \beta u a). \end{aligned}$$

We distinguish three cases:

1. Let $\bar{y} := \text{prox}_{\beta\varphi}(x^0 - \beta a)$ and suppose that $c + \langle a, \bar{y} \rangle > 0$. Then $\partial(\cdot)_+(c + \langle a, \bar{y} \rangle) = \{1\}$ and hence \bar{y} satisfies (37) with $u = 1$. Hence, $y^+ = \bar{y}$.

2. Let $\bar{y} := \text{prox}_{\beta\varphi}(x^0)$ and suppose that $c + \langle a, \bar{y} \rangle < 0$. Then $\partial(\cdot)_+(c + \langle a, \bar{y} \rangle) = \{0\}$ and hence \bar{y} satisfies (37) with $u = 0$. Hence, $y^+ = \bar{y}$.
3. If neither the condition of the first nor of the second case of (36) are satisfied, then, as (37) is a necessary condition for the solution y^+ , it must hold $c + \langle a, y^+ \rangle = 0$. Hence, there exists a $u \in \partial(\cdot)_+(c + \langle a, y^+ \rangle) = [0, 1]$ such that

$$c + \langle a, \text{prox}_{\beta\varphi}(x^0 - u\beta a) \rangle = 0.$$

□

Lemma 13. *For any $K \geq 1$ it holds*

$$\begin{aligned} \sum_{k=0}^{K-1} \frac{1}{k+1} &= 1 + \sum_{k=1}^{K-1} \frac{1}{k+1} \leq 1 + \int_0^{K-1} \frac{1}{s+1} ds = 1 + \ln K, \\ \sum_{k=0}^{K-1} \frac{1}{\sqrt{k+1}} &\geq \int_0^K \frac{1}{\sqrt{s+1}} ds = 2\sqrt{K+1} - 2. \end{aligned}$$

C Model equivalence for SGD

In the unregularized case, the SGD update

$$x^{k+1} = x^k - \alpha_k g_k, \quad g_k \in \partial f(x^k; S_k),$$

can be seen as solving (5) with the model

$$f_x(y; s) = f(x; s) + \langle g, y - x \rangle, \quad g \in \partial f(x; s).$$

Now, consider again the regularized problem (2) with $\varphi(x) = \frac{\lambda}{2}\|x\|^2$ and update (8).

On the one hand, the model $\psi_x(y; s) = f(x; s) + \varphi(x) + \langle g + \lambda x, y - x \rangle$ with $g \in \partial f(x; s)$ yields

$$x^{k+1} = x^k - \alpha_k(g_k + \lambda x^k) = (1 - \alpha_k \lambda)x^k - \alpha_k g_k. \quad (38)$$

On the other hand, the model $\psi_x(y; s) = f(x; s) + \langle g, y - x \rangle + \varphi(y)$ with $g \in \partial f(x; s)$ results in

$$x^{k+1} = \text{prox}_{\alpha_k \varphi}(x^k - \alpha_k g_k) = \frac{1}{1 + \alpha_k \lambda} [x^k - \alpha_k g_k] = (1 - \frac{\alpha_k}{1 + \alpha_k \lambda} \lambda)x^k - \frac{\alpha_k}{1 + \alpha_k \lambda} g_k. \quad (39)$$

Running (38) with step sizes $\alpha_k = \beta_k$ is equivalent to running (39) with step sizes $\frac{\alpha_k}{1 + \alpha_k \lambda} = \beta_k \iff \alpha_k = \frac{\beta_k}{1 - \beta_k \lambda}$. In this sense, standard SGD can be seen to be equivalent to proximal SGD for ℓ_2 -regularized problems.

D Additional information on numerical experiments

D.1 Matrix Factorization

Synthetic data generation: We adapted the experimental setting of the deep matrix factorization experiments in (Loizou et al., 2021), but extending with regularization. We generate data in the following way: first sample $B \in \mathbb{R}^{q \times p}$ with uniform entries in the interval $[0, 1]$. Then choose $\kappa \in \mathbb{R}$ (which will be our targeted inverse condition number) and compute $A = DB$ where D is a diagonal matrix with entries from 1 to κ (equidistant on a logarithmic scale)¹⁰. In order to investigate the impact of regularization, we generate a noise matrix E with uniform entries in $[-\varepsilon, \varepsilon]$ and set $\tilde{A} := A \odot (1+E)$. We then sample $y^{(i)} \sim N(0, I)$ and compute the targets $b^{(i)} = \tilde{A}y^{(i)}$. A validation set of identical size is created by the same mechanism, but computing its targets, denoted by $b_{\text{val}}^{(i)}$, via the original matrix A instead of \tilde{A} . The validation set contains $N_{\text{val}} = N$ samples.

¹⁰Note that (Loizou et al., 2021) uses entries from 1 to κ on a *linear* scale which, in our experiments, did not result in large condition numbers even if κ is very small.

Name	p	q	N	κ	r	ε
matrix-fac1	6	10	1000	1e-5	4	0
matrix-fac2	6	10	1000	1e-5	10	0.05

Table 1: Matrix factorization synthetic datasets.

Model and general setup: Problem (28) can be interpreted as a two-layer neural network without activation functions. We train the network using the squared distance of the model output and $b^{(i)}$ (averaged over a mini-batch) as the loss function. We run 50 epochs for different methods, step size schedules and values of λ . For each different instance, we do ten independent runs: each run has the identical training set and initialization of W_1 and W_2 , but different shuffling of the training set and different samples $y^{(i)}$ for the validation set. In order to allow a fair comparison, all methods have identical train and validation sets across all runs. All metrics are averaged over the ten runs. We always use a batch size of 20.

D.2 Plots for matrix-fac2

In this section, we plot additional results for Matrix Factorization, namely for the setting `matrix-fac2` of Table 1. The results are qualitatively very similar to the setting `matrix-fac1`.

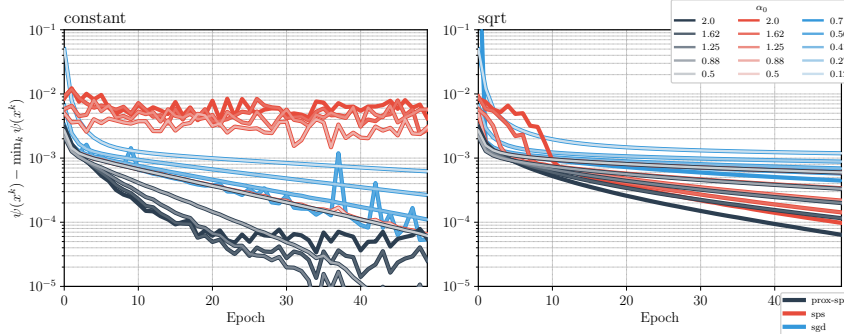


Figure 10: Objective function for the Matrix Factorization problem (28), with `constant` (left) and `sqrt` (right) step size schedule and several choices of initial values. Here $\min_k \psi(x^k)$ is the best objective function value found over all methods and all iterations.

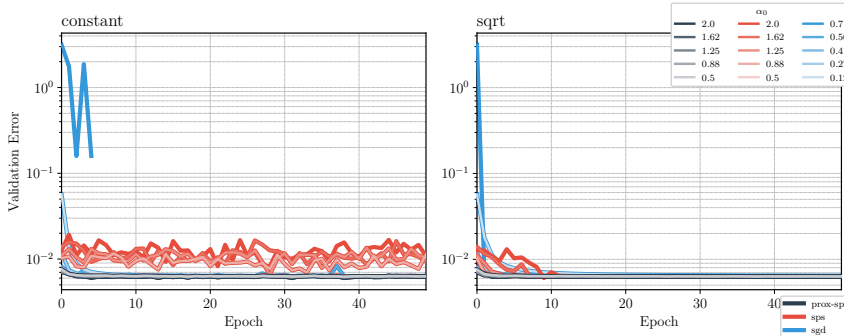


Figure 11: Validation error for the Matrix Factorization problem (28), with `constant` (left) and `sqrt` (right) step size schedule and several choices of initial values.

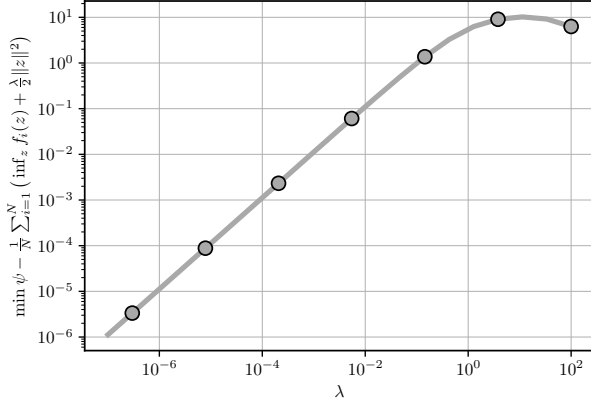
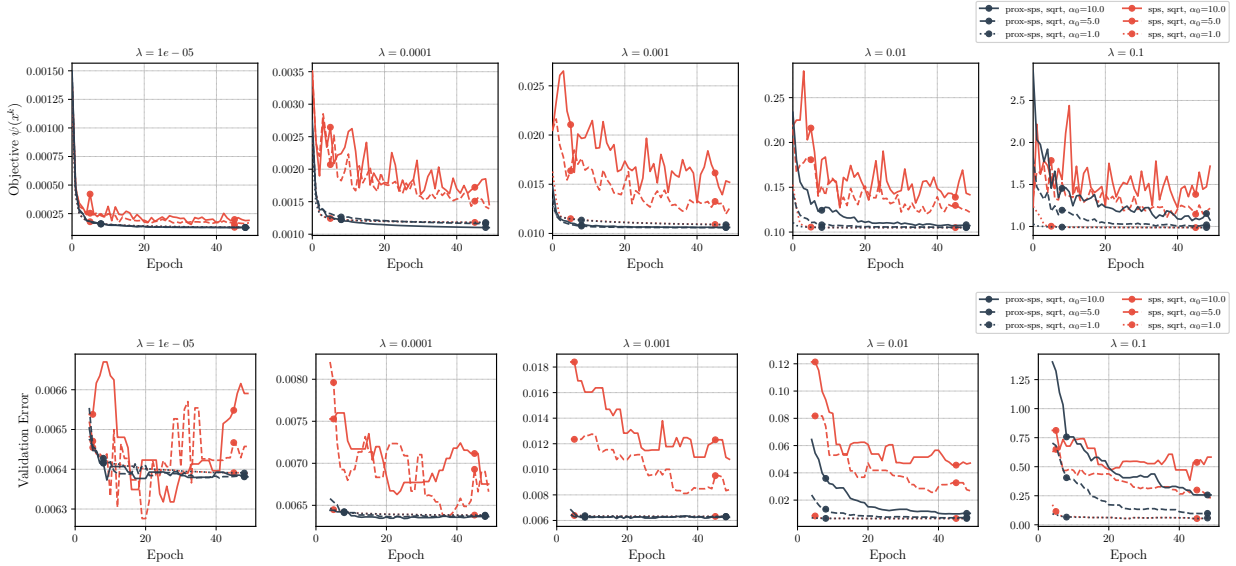
Figure 13: Interpolation constant for a ridge regression problem for varying regularization parameter λ .

Figure 12: Objective function value and validation error over the course of optimization. For the validation error, we plot a rolling median over five epochs in order to avoid clutter.

D.3 Interpolation constant

We illustrate how the interpolation constant σ^2 behaves if it would be computed for the regularized loss $\ell_i(x) = f_i(x) + \frac{\lambda}{2} \|x\|^2$ (cf. also Section 4.2). We do a simple ridge regression experiment. Let $A \in \mathbb{R}^{N \times n}$ be a matrix with row vectors $a_i \in \mathbb{R}^n$, $i \in [N]$. We set $N = 80$, $n = 100$ and generate $\hat{x} \in \mathbb{R}^n$ with entries drawn uniformly from $[0, 1]$. We compute $b = A\hat{x}$. In this case, we have $f_i(x) = \frac{1}{2}(a_i^\top x - b_i)^2$ and $f(x) = \frac{1}{N} \sum_{i=1}^N f_i(x)$.

If one would apply the theory of SPS_{\max} for the regularized loss functions ℓ_i with estimates $\ell_i = 0$, the constant $\sigma^2 = (\min_{x \in \mathbb{R}^n} f(x) + \varphi(x)) - \frac{1}{N} \sum_{i=1}^N \inf_z \ell_i(z)$ determines the size of the constant term in the convergence results of (Loizou et al., 2021; Orvieto et al., 2022). We compute $\min_{x \in \mathbb{R}^n} f(x) + \varphi(x)$ by solving the ridge regression problem. Further, the minimizer of ℓ_i is given by $(a_i a_i^\top + \lambda \text{Id})^{-1} a_i b_i$. We plot σ^2 for varying λ in Fig. 13 to verify that σ^2 grows significantly if λ becomes large (even if the loss could be interpolated perfectly, i.e. $\inf_x f(x) = 0$). We point out that the constant σ^2 does not appear in our convergence results Theorem 7 and Theorem 8.